8-2016

Validating the Operating Window Concept for Robustness on a Circuit Board Stencil Printing Process

Wagner Pereira Romito
wpr4207@rit.edu

Validating the Operating Window Concept for Robustness on a Circuit Board Stencil Printing Process

by

Wagner Pereira Romito

Thesis submitted in partial fulfillment of the requirements for the

Degree of Master of Science in Manufacturing and Mechanical System Integration

Rochester Institute of Technology

College of Applied Science & Technology

Department of Manufacturing and Mechanical System Integration

August, 2016

Rochester Institute of Technology

College of Applied Science & Technology

Master of Science in Manufacturing and Mechanical System Integration

Thesis Approval Form

Student Name: Wagner Pereira Romito

Thesis Title: Validating the Operating Window Concept for Robustness on a Circuit Board Stencil Printing Process

Thesis Committee

Name	Signature	Date
Dr. James Lee Chair		
Dr. Robert Garrick Committee member		
Dr. Marcos Esterman Committee member		

"O objetivo fundamental dos sonhos não é o sucesso,
mas nos livrar do fantasma do conformismo."

– Cury, O Vendedor de Sonhos, 2009

To my parents, Paulo and Marli.

Acknowledgments

I am thankful to everyone who contributed, directly or indirectly, with the development of this research.

I acknowledge my advisors for the opportunity and support that ledge to the completion of this project.

To the MMET department and all the faculty members that provided the tools to build and improve my knowledge.

To the Rochester Institute of Technology (RIT) for the amazing reception and structure that enabled the development of this research in a soundly manner.

I would like to thank CAPES/CNPq for funding my master program under the Brazilian Scientific Mobility Program (Ciências sem Fronteiras), process number 88888.076031/2013-00.

To Jeffrey Longville and Tayler Swanson from the CEMA lab, for supporting me on the experimental phase of this research.

I am thankful to QVI, specially Ken Sheehan, for opening the doors of their company and providing access to their metrology machinery.

I specially thank my friend and partner Ana Carolina Pessôa, to encourage me to embark on this journey.

To my grandparents, because they have not measured efforts to always give me the best education.

To all my family for all the love and support that was the foundation that enable me to pursue my dreams.

And finally for all my Brazilian friends that shared these two years as a great family.

To all, honestly, my gratitude!!

Abstract

The lifecycle of a system is dependent on the system design. However, the concern with quality has been stressed mostly during its production and use. The understanding of the system variability generated by noise variables shifted the quality focus to the design phase. The development of robustness early on the system lifecycle increases the system reliability through its entire life cycle. Although the robust design approach developed by the Taguchi methods application had a great contribution to this philosophy, there is much criticism of this methodology. One alternative to the Taguchi method is the Operating Window methodology. Its application has successfully been demonstrated as a substitute for the Taguchi methods, especially when the response is not quantitative. However, most of the examples were used repeatedly and the steps on the application of the methodology have not been well detailed. Therefore, this project had the objective of developing a unique application of the methodology with a simple approach. Moreover, with the implementation of the methodology, the project aims to identify the difference between a design with a wide output data distribution and a design with a narrow distribution. The methodology followed the Operating Window methodology steps, applying it to a circuit board printing process. The results have shown that it is possible to have a relationship between the Operating Window range and the distribution variation from the system output.

Table of Contents

List of Figures

List of Tables

Table of Abbreviations

AR	Area Ratio
CEMA	Center for Electronics Manufacturing and Assembly
CAD	Computer-Aided Drafting
FAMe	Failure Amplification Method
FTA	Fault Tree Analysis
Gage R&R	Gage Repeatability and Reproducibility
LD50	Half of the Lethal Dose
in	Inches
nl	Nanoliters
lbs	Pounds
PCB	Printed Circuit Board
SMT	Surface Mount Technology
TRIZ	Theory of Inventive Problem Solving
TE	Transfer Efficiency
01005	Components with 0.1”x0.05” size

Validating the Operating Window Concept for Robustness on a Circuit Board Stencil Printing Process.

Introduction

Quality control is performed to guarantee that the process will produce products as expected. The process is controlled as to not allow the production of products outside the customer requirement limits. Although final inspection is known to be used as a ineffective attempt to avoid bad products from being delivered to the customer (Juran & Godfrey, 1998), companies still use this quality assurance procedure alone. However, the main quality efforts should be focused on assuring that the process is capable of producing within the customer requirements during its life cycle. The reason that final inspection should be avoided is that it is performed at the end of the process, when the product has already been produced and the defects have already been generated at some earlier point in the process. This means that if any fail to meet the customer specification is detected at this point, it will result in more costly production waste. The costs of rejecting a product after it has been produced are greater than the cost of preventing the nonconformance (Juran & Godfrey, 1998; Crosby, 1979). Moreover, when this inspection system fails and a defective product is not detected, the consequences are even greater.

As process capability is mainly a measurement of the effects of variability on the process, efforts should be made to reduce the process variability (Gryna, Chua, De Feo, & Juran, 2007). An alternative approach to controlling variability during the entire life cycle is to engineer the product or process to be robust enough to account for this variability (Clausing, 2004). Although the first is the most common approach, the development of process robustness is the more

effective approach (Clausing, 2004). Quality efforts in companies have been developed to fix problems related to production. Programs such as Six Sigma have been heavily developed to control the occurrence of production problems (McClusky, 2000). Although the success of these methodologies has been proven, the design of a process resistant to noise would eliminate the need for such process control approaches. In other words, the lack of process robustness creates the necessity to develop problem-solving programs such as Six Sigma in order to reduce the effects of noise variables on the production system (Clausing, 2004).

Solving product problems and solving process problems are different in nature and can lead to different consequences. In many cases, even when a process is not effective, it can be adjusted and changed before the final product is produced. However, a product cannot be fixed after it was already delivered to the customer without greater consequences (Feigenbaum, 1991). This is true as customers expect the product functionality to be reliable during its entire life cycle (Yang, 2007). The consequences could be financial or related to customer satisfaction (Juran & Godfrey, 1998). Satisfaction of the customer is the key factor to a company's success. Because of the need to achieve customer satisfaction, products have to be designed to maintain its performance as expected during its entire life cycle (Bergman, de Mare, & Svensson, 2009; Schenkelberg, 2013). This is achieved by designing performance robustness into the product.

Robustness is achieved by making a system insensitive to noise effects. The introduction of the robustness concept into the design phase is a key to designing a system able to meet customer requirements under different operating conditions (Clausing, 2004). Robust design can be useful for both product and process development. Many times in new product development, the process is not capable of yielding the expected results to produce the product under development (Hoyle, 2005). The manufacturing process might need to be modified if the new

product characteristics exceed the existing process capability. However, these changes might increase the development cost and time. In addition, machinery restrictions might hamper the product development when the product characteristics exceed the machine limits. To assure quality, things have to be done right from the first time (Crosby, 1979). This suggests that a process needs to be developed considering all possible applications during its life cycle. A process robust to changes on its main functions is necessary to enable the use of new configurations on the product development procedure.

The robust design methodology gained large scale adoption through Taguchi's development and implementation of an experimental design methodology often referred to as Taguchi methods (Roy, 2010). However, Taguchi's approach has also been critiqued (e.g. Nair et al. 1992) and new methodologies have been developed to address the problems identified in the Taguchi methods. The Operating Window concept is one example. Although the Operating Window methodology has been studied on some examples (Fowlkes & Creveling, 1995; Mori, 1995; La Vallee, 1992; and, Peace, 1993) there is still a need to further develop the methodology. Among these are the need to better define the steps to apply the methodology in practice and the need to develop more examples of its application. For instance, the paper feeder subsystem (La Vallee, 1992) and the wave soldering process (Peace, 1993) are the two main examples that have been used in the operating window research. Considering the importance of developing robustness of a system early in its development and the problems identified with Taguchi methods, this research will apply of the Operating Window methodology to the development of process robustness.

In this work, the Operating Window methodology was applied to test the hypothesis that designs with a wider distribution have a smaller operating window as compared to designs with a

narrower distribution. A large variation means that the specific configuration presents small capability of performing under acceptable conditions. On the other hand, configurations with a small variation have a greater probability of meeting performance specifications. Therefore, designs with smaller variations should outperform designs with large variations in terms of capability. In addition, designs with narrow distributions should be less sensitive to noise effects; hence these designs should have a greater level of robustness when compared to designs with wider distributions.

The remainder of this thesis is organized as follows: Literature Review, Project Objectives, Methodology, Analysis and Results, and Conclusions. The first Chapter will summarize the literature used as a source of knowledge for the development of this study. It contains the theoretical framework that guides and justifies this research. And, it will identify the gaps on previous research. The second Chapter will propose the objective to fill the identified gaps. The third Chapter presents the methodology used in the project. It covers the definition of the study universe, the instruments used, how the data was collected and analyzed, as well as its limitations. It will explain how the objectives will be achieved. The fourth Chapter will present the experimental results and findings. Finally, the fifth Chapter presents the conclusion of the research, summarizing the findings and learnings as well as presenting suggestions for future studies.

Literature Review

In this section, a review of related literature will be presented. First, an overview of robust design will be presented, which will describe its role in the product life-cycle, present a review of Taguchi methods and the critical role that the noise plays. In addition, since the definition of limits and boundaries is such an important part of the operating window concept, a

review of tolerance design is included. Finally, a detailed review of the Operating Window concept is included, which includes its previous applications, and the definition of failure boundaries through failure modes analysis and the analysis of the system physics.

Robust Design

Robustness is defined by Clausing (2004) as the system's capacity to perform as expected even under the effects of noise factors. A new system has to be able to produce the same results in different operating conditions. This adaptability is defined as robustness and is achieved through the adjustment of the technology variables (Taguchi, 1993). The concept of robustness represents the intrinsic system setup that allows the system to function as expected even under the presence of some disturbance that could harm the system operation. A process is considered robust when changes in the production environment do not affect the production quality. The process continues to produce within the tolerance limits even when those changes are present.

Systems are developed based on previous systems performance. Incremental changes are implemented to overcome identified problems on previous versions by adding new features to the system. This problem-solving approach is a major problem of the traditional system development. It is a good approach to solve emergency or small problems but it fails to eliminate the root cause of the problem. Robustness is the right approach to eliminate the problem by reducing variance (Clausing & Fey, 2004). Problems are consequences of the system functions variance. Large variations generate system malfunctions. The development of system robustness reduces the variance and, consequently, reduces the probability of problems to occur. Robust design methods to reduce variance have had great success to improve reliability in addition to quality and consequently this leads to customer satisfaction (Meeker and Escobar, 2004b).

Robustness is part of reliability improvement of a system by avoiding failure modes and it should be developed early in the design stage when modifications are cheaper (Clausing, 2004) and less restricted. Robust design aims to optimize the relationship between control variables and output responses (Mori & Tsai, 2011) it enhance a system's quality and reliability, reduces warranty costs and customer service costs, speeds up the time to market, and reduces development costs (Clausing & Fey, 2004).

Product lifecycle. The design process is a phase of the product lifecycle as is shown in Figure 1. The design phase is a systematic process that conceptualizes a new system. Innovations or customer needs are translated into the activities necessary to produce the new system. The design phase identifies the real market needs, defines the system's functions and its requirements, defines the product specifications, and identifies the process variables necessary to produce that product (Wallace & Clarkson, 1999).

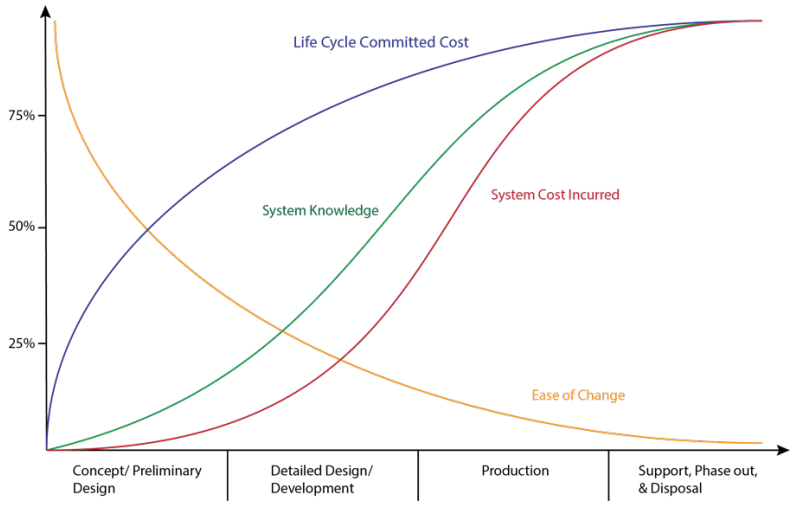

Figure 1. Product Lifecycle Cost. This figure illustrated the product lifecycle phases and costs. Adapted from" Systems engineering and analysis." by Blanchard, B. S., & Fabrycky, W., 2010.

The concern with fast customer satisfaction prejudices the design phase of a system development. The design focus is changed to a short-term concern and the consequences of the

changes are not fully analyzed. This lack of proper planning generates problems that will need to be fixed late in the development phase. The design decisions need to be based on the entire system lifecycle (Blanchard & Fabrycky, 2010).

The design phase enables development cost reduction. Figure 1 shows that changes early in the design phase are less expensive to implement and have a big impact on the reduction of the system life cycle cost. This is true because late in the development process, the decisions that were taken earlier committed to these downstream costs (for example, an inexpensive yet unreliable design selected early in the design phase, could lead to a larger number of product development testing failures, manufacturing defects and field failures). This situation emphasizes the importance of early design decisions. However, Figure 1 shows that current practices of delaying design decisions and cost commitment can increase the system development costs (Blanchard & Fabrycky, 2010).

In addition to the life cycle cost reduction opportunity, the development of robustness early in the design phase reduces the time of subsequent activities and consequently the product time-to-market. However, some concern has to be taken not to spend too much effort achieving robustness and missing the time-to-market (Clausing & Fey, 2004).

Taguchi methods. Product development used to follow a trial and error approach (von Hippel, 1998). On a trial and error practice, robustness was improved by identifying how to break a component, then making the component harder to break. Failure was identified and typically, a one factor at a time approach for experimentation was followed. Several trials were necessary for this approach and the performance of output response was limited to a target determined before the experiment (Mori & Tsai, 2011). However, as is stated by Clausing and

Fey (2004), system robustness is achieved more quickly by analytical methods as opposed to experimental methods.

Taguchi (1986) was the precursor of this philosophy with the development of methods to increase system robustness. The Taguchi method is defined by two-step to maximize the signal to noise ratio in order to meet the customer's requirements. The first step minimizes the system variability under operating conditions, making the system robust to noise. It is achieved by varying the system variables in order to achieve the appropriate signal to noise ratio. After the system is made robust, the second step consists of bringing the parameters close to the values specified by the customer. Taguchi (1993) defends that is it not possible to focus only on the customer requirements. Once the system is under operating conditions it has to be robust to yield the expected result that was obtained under controlled conditions.

As it is explained by Roy (2010), the Taguchi method uses orthogonal arrays to create experimental protocols that facilitate the analysis of system performance. It is composed of an inner array that contains the system control parameters levels used in the experiment and, if the noise variables have been identified and can be controlled, by an outer array with the noise variables levels. Table 1 shows an example of orthogonal arrays. The inner array is often a fractional factorial array used to estimate the main effects, as these types of factorials have confounded factors in its alias structure. This mean that the it is not possible to estimate each factor effect separately. The estimated effect will be the sum of the effects of the two or more factors that are considered confounded. The relations of all factors are defined on the alias structure. Each row of the inner array represents a system configuration that will be used to run the experiment. The results obtained on the experiment are filled in the outer array. Each

column of the outer array represents the noise condition in which the runs will occur. The analysis is made with these responses' means and by a signal to noise ratio (Roy, 2010).

Table 1

Taguchi method generic example.

	Inner Array			Outer Array			
Runs	Factor 1	Farctor 2	Factor 3	Response values under Noise condition 1	Response values under Noise condition 2	Mean Response	Signal to Noise Ratio
1	1	1	2	10	20	15	6.53
2	1	2	1	13	23	18	8.12
3	2	1	1	14	26	20	7.45
4	2	2	2	5	11	8	5.51

The signal to noise ratio is a measurement of variability created by the noise variables as can be seen in Table 1. This performance measurement is the ratio of the quality factor effect to the noise factor that influences the signal. The use of the signal to noise is made through a logarithm transformation as can be seen on Equation 1. The measurement efficiency is improved by the logarithm transformation as it increases the additivity of the input variables over the output response (Mori & Tsai, 2011). The signal to noise ratio is a measurement that can be applied to different types of technology but it does is not a comparable measurement (Taguchi, 1993). It is not possible to state that a product is more robust than a different product by just comparing their signal to noise ratio.

$$\mathrm{S/N} = 10 \log\left(\frac{\bar{y}^2}{s^2}\right) \quad (1)$$

Taguchi (1986) applied a quantitative method to deal with robustness through the signal to noise ratio. Although the Taguchi approach have the advantage of relying on quantitative data, in some circumstances, the collection of continuous data is not possible or not affordable. Sharma and Cudney (2009) identified that the methodology developed by Taguchi (1986) was not balanced. In terms of the operating window, the methodology applied distinct statistical transformations at each of its limits, generating a higher impact on the lower limit. Because of this problem a new methodology was proposed to provide more realistic outcomes to the optimization process. Joseph and Wu (2002) considered that the model developed by Taguchi (1986) was functional under restricted assumptions. A more flexible model was developed by the application of general linear functions and a two-step approach for optimization.

Noise. During the innovation process, a new system might work well in a laboratory environment, however, its performance changes during production, because of uncontrollable variables inherent in the process. The changes in the product performance during production that differ from those in a controlled environment (typical under ideal conditions) is caused by noise (Clausing & Fey, 2004). Noise is defined as the non-controllable variation in a functional parameter, critical for the system performance. (Clausing, 2004).

The function of a system can be divided into two parts, first is the optimal function of the system defined as useful part. The second is the effects of noise variables over the function defined as harmful part (Taguchi, 1993). The noise increases the probability of a failure mode to occur (Clausing, 2004) as it increases the variation in the system performance. Variation in the product characteristics are a reflection of noise. These variations include (Clausing & Fey, 2004):

- Environmental variation:
    - External environmental variation
    - Customer-use profile
    - Interactions with other subsystems and components.
- Variations in the product characteristic:
    - Variations in production: Noise to the designers. Variation in production affects the system performance. However, if the system is robust, the production variations will not have a high influence on the system performance.
    - Variations as the result of time and use, it includes wear and deterioration.

Noise is the cornerstone of the operating window methodology. It is applied as a factor to increase the system's variation and is used to measure system's robustness through the critical parameter variation (Clausing, 2004). Armillotta and Semeraro (2013) also highlight the importance of studying functional requirements in the presence of noise early in the design phase. Functional Noises are defined as functional variables that control the physics of the product main functions. The system is made more robust by controlling these variables (Clausing & Fey, 2004).

Tolerance Design

Tolerances are the limits that allow a parameter to assume different values (Creveling, 1997). The nominal value of a parameter is usually defined during the design stage. However, as Bernardo and Saraiva (1998) suggest, this definition often ignores the control phase that will use the defined value. Ignoring the parameter control by defining a single nominal value instead of a variation range, the defining effort fails to address noise that will be present in operation conditions. The production noise variables will preclude the parameter from being at its nominal

value. Creveling (1997) argues that the tolerance limits should be conceived in the design stage, based on the customer perception or the system function.

The specification of tolerance limits has the objective to protect a system's main function from deviating from its expected outcome. For example, to prevent the system from operating outside its specified limits and generating safety issues. In other words, the nominal value is seen as a target but there is a range of values that yields acceptable quality levels. The threshold of this interval is identified by changing the systems variables until a failure occur (Taguchi, 1993). The tolerance design decision, in Taguchi's (1993, pp. 39) opinion, should be "based on the trade-off between the average quality loss function and the average cost of products". The tolerance interval of control variables reduction cause the control cost to increase (Bernardo & Saraiva, 1998).

Often a safety factor is necessary to assure that the variation during production does not let to the production of a defective system (Taguchi, 1993). The necessity of this safety factor exists because the product development process occurs in a controlled environment. When the developed system is placed under operating conditions, it experiences the effects of noises that were not present in its development. Such noises can make its functions' variability increase to levels that might take it outside of its requirement limits.

Tolerances are identified taking into account variations from the mean value of a specific design parameter. However, there is a need to account for all operation factors inherent to the system when the design parameter variance is defined (Armillotta & Semeraro, 2013). The operating window will serve this purpose.

Operating Window

Herron, Hodgson, and Cardew-Hall (1998) defined operating window as the operating limits that consider the variables of a process as a single system. In other words, the operating window can be thought as the boundaries of a system a critical parameter where after, failure modes are more likely to occur (Joseph & Wu, 2002). Clausing (2004) identified the operating window as a robustness metric that is easily measured in practice and that is directly related to the prevention of a system's identified failure modes occurrence. Operating window is a range of values that the operating parameters meet the specified functional parameters (Armillotta & Semeraro, 2013) yielding the best results in economic and quality terms (Bernardo & Saraiva, 1998).

The operating window upper and lower boundaries are defined as failure limits. A two dimensional operating window is bounded by failure modes on both sides (Joseph & Wu, 2002). For this reason, a system's critical parameter has to avoid these boundaries. The critical parameter has to be small enough to reduce the probability of failure from the upper limit, but has to be large enough to minimize the probability of failure from the lower limit (Sharma & Cudney, 2009). The critical parameter can safely obtain values inside this range. However, mostly due to noise, variability may increase the probability of failures modes. Sharma & Cudney (2009) explains that one can increase the range of values that the critical parameter can obtain by widening the operating window limits. This fact makes the systems more robust due noise variation. So, the larger the operating window, more robust is the system.

The objective of the operating window approach is to make the product robust early in the design phase by inducing high failure rates through changes in operating parameters and the application of noise. Clausing (2004) noted that typically efforts to increase robustness are

executed late in the development phase where the ability to make changes is restricted and a large number of trials are needed to assess small failure rates. In response to that, the operating window uncovers robustness problems early in the design phase with fewer trials. This is possible by inducing high failure rates early in the design phase and using noises factors to excite the failure modes. The large amount of noise applied, makes the system development to consider a scenario closer to the real operating environment (Clausing & Fey, 2004).

The difference is that the product will be developed under the effects of noise instead of dealing with this effect only in the production phase and having a high chance of failure (Clausing & Fey, 2004). Early in the product development phase, the systems are typically developed under controlled conditions just to prove that its performance can be superior to a previous model. However, with the introduction of the operating window concept, what will be discovered is that the operating window is narrow or even negative as the system will be vulnerable to failure modes in operational conditions. But it is the early introduction of this noise and the excitation of these failure modes that enables the system control variables to be defined and enables learning from failure, which ultimately leads to a more robust product. This increase in robustness is directly linked to the opening of the operating window (Clausing & Fey, 2004).

The system operating window is defined after the understanding of the system function, its failure modes, and the noise that generate them. Clausing and Fey (2004) explain the process by first setting the system with its best know operating parameters. The second step consist of inputting a fixed noise variable and adjusting the operating window variable to have a high failure rate, generally, 0.5. The process is repeated for the other side of the operating window. The experiment start with the severe noise imputed at a moderate level. After the operating

window is opened, the noise level is increased to further improve the operating window. The best approach is not yet defined. But the main concept behind the operating window approach, independent of the method used, is the understanding of the system physics (Clausing & Fey, 2004).

The identification of the operating window is a quite simple task given a single or two system critical parameters (Armillotta & Semeraro, 2013; Clausing, 2004). However, a multidimensional set of requirements increases its complexity becoming a difficult task for product designers (Armillotta & Semeraro, 2013). Operating window for a single critical factor is easily defined and achieved. However, systems usually have more than one critical factor but few examples have been studied (Clausing & Fey, 2004).

The development of robustness through the operating window has to be gradual. Starting with a moderate level of noise then increasing after the operating window is found and expanded for each level. The expansion of the operating window is made based on the system control parameters. This approach would make the system robustness to constantly increase for the initial noise level (Clausing, 2004). The result of the operating window process is the definition of the set of design parameters that yield the best result to the system and its tolerances. The level of these parameters are set as a requirement for the next activities until the final commercial concept is developed (Clausing & Fey, 2004).

Compared to Taguchi (1986) approach, the operating window is easier to be applied by the development team as it is more intuitive in terms of engineering (Clausing & Fey, 2004). The operating window is developed exploring the system physics and allows the robustness development without quantitative experimental results. Taguchi (1993) stated that the operating window method is more suitable for qualitative data. Although continuous data allow the

experimenter to obtain more information, categorical variables are easier to obtain and can be converted to other measurements as pecuniary (Joseph & Wu, 2004).

Although the measurement of the system robustness is better achieved through the identification of a functional attribute, it is a difficult task to identify or measure the appropriate functional attribute (Joseph & Wu, 2002). Joseph and Wu (2002) identified the use of the operating window as an opportunity to deal with the functional attribute problem by identifying a single "operating window factor" to define the limits of which failure modes are likely to affect the system. Because the operating window defines the limits where a systems critical parameter could vary without failures, to deal with noise, it would be reasonable to think of enlarging those limits and make the system more robust (Joseph & Wu, 2002).

The Taguchi method first identifies the value that yields a better outcome in terms of robustness then the tolerances are calculated based on this value. The operating window method has the opposite sequence. It first identifies the thresholds values for the operating window. After the limits are identified, the set point is defined taking into consideration the distance from the limits and the severity of the failures at each boundary. The identification of the operating window generally occurs by looking at the thresholds separately. One signal to noise ratio is developed for each limit. For the lower boundaries it assumes a smaller the better property and for the upper boundaries a large the better characteristic. The operating window signal to noise ratio is the sum of the thresholds signal to noise (Taguchi, 1993).

The operating window is identified by Taguchi (1993) as a methodology to develop robustness in a new technology in an efficient way. It allows improving robustness in a reduced quantity of development cycles and cost compared to traditional approach. Clausing (2004) observed that the parameter employed to assess the robustness of a system is of a greater

importance than the method used to identify the range of control parameters where the higher level of robustness is achieved.

Previous application. Many industries do not have full knowledge of how their production systems work and this knowledge is usually concentrated within employees with more experience. However, in a dynamic environment with changing product needs, these experienced employees also face a lack of knowledge to adjust the machines to produce new products (Herron et al., 1998). Herron et al. (1998) identified the need to understand a system's operating window and to develop an interaction framework. The employees that setup the machine, uses the operating window to predict the response of the inputs.

The motivation of the operating window methodology is that initial manufacturing tolerance is not capable of maintaining a critical factor within the operating window. With the development of the methodology by progressively widening the limits of the failure modes, the manufacturing tolerance in turn become more capable and even robust enough to maintain the critical factor within its desired levels (Clausing, 2004). Herron et al. (1998) also noted that in certain cases, even when the quality of a supply varies it takes less time to set up a machine taking account the noise instead of sampling the supplies. Eliminating the noise is not always feasible or requests a higher investment making manufacture companies to have to deal with these situations. As Sharma and Cudney (2009) concluded, the operating window concept can be applied to increase the product or process robustness, in addition to being useful for management decisions.

Joseph and Wu (2004), developed a methodology known as failure amplification method (FAMe) based on the same principles of the Operating Window. In the methodology, an amplification factor is selected, based on engineering knowledge of the system, in order to excite

the failure modes. However, they apply this approach using three different factors: Control Factors, Complexity Factors, and Noise Factors. Complexity factors are defined as factors defined by the customer specification that limits the product manufacturing (Joseph & Wu, 2004). The Operating window is considered as a special case of the FAMe when two distinct functional characteristics generate two different failure modes (Joseph & Wu, 2004). Because of the difficulty to identify and measure these functional characteristics, it is necessary to interpret their function based on the failures categorical data.

Failure Boundaries

Failure modes. A deviation of a system's ideal functionality can be thought of as a failure mode from a customer's perspective (Clausing, 2004). Failures are defined by Joseph and Wu (2002) as boundaries of a system's functional parameter. These failure boundaries create an interval in which the system is functional. The problem of working in a limited interval is that avoiding either limit separately is easily achieved, however when both limits a taken into account a greater effort is needed. In addition, the failure modes might be correlated. If this is true, all of them are needed to be analyzed at the same time (Clausing, 2004). Moreover, the correlation of the failure modes might generate trade-offs to increase the system robustness. These trade-offs are often related to a theory of inventive problem solving (TRIZ) physical contradiction of the operating window (Clausing & Fey, 2004).

Control variables and noises that affect the system functional parameter are directly related to failure modes probabilities (Armillotta & Semeraro, 2013). In the operating window method, each failure mode is excited by the introduction of a correlated noise variable. The objective is to identify the system control variables setting that avoid the effect of a failure to the system.

Failure to perform the system basic function has to be considered the main focus of new product development. Failure modes that are side effects of the primary failure are controlled by defining limits levels for the function as a design constraint. In addition, failures modes that induces fails to a system' physical part are mitigated by design changes and material selection (Clausing & Fey, 2004).

System physics. The identification of the critical function variables is the first step in the development of robustness. To identify these variables is necessary to understand the system physics. With the understanding of the parts' interactions, it is possible to identify the critical variables that are also easy to adjust. This process is facilitated by the use of reliability tools. i.e. Fault Tree Analysis (FTA) (Clausing & Fey, 2004).

The relationship between a factor and its effects on failure modes is heavily dependent on the knowledge of the system physics. However, it might be difficult to physically identify this relationship (Meeker and Escobar, 2004a), adding difficulties to expanding the Operating Window. To deal with this issue, experimental designs are needed. In an experimental development, it is necessary to have a representation of the system including the realistic physics of the system concepts and the adjustable critical function variables (Clausing & Fey, 2004). This system representation will enable the study of the input-output interactions, essential for the system optimization (Mori & Tsai, 2011).

Project Objectives

The main objective of this project is to evaluate the performance of the operating window methodology. This will be achieved by applying the operating window concept to a circuit board printing process. An experiment will be used to identify which of the possible process designs represent the best robustness performance and which represent the worst. The results of this experiment, will be used to test the hypothesis that the design with the smallest variation had the widest operating window and, conversely, the one with the largest variation has the narrowest operating window.

The following are the specific objectives of this work:

i) Implement the operating window methodology on the stencil printing of circuit boards.

ii) Replicate the experiment from Mohanty, Ramkumar, Anglin, Oda, and Mark (2011).

iii) Identify the critical parameters, failure modes, and noise effects that are governed by the systems physics.

iv) Define the type of operating window to be used based on the critical parameters, failure modes and noise effects identified.

v) Select the process designs that have the best and worse performance in terms of variation.

vi) Verify the hypothesis that a design with a wider distribution has a smaller operating window compared with a design with a narrow distribution.

Methodology

The project will be developed based on the seven steps proposed by Clausing and Fey (2004) to successfully apply the operating window concept. These steps consist of:

i) Identify the system critical functional variables through the analysis of the physics of the system.

ii) Define the resources to be used on the development of robustness. The resources have to represent the system and have to allow changes on the critical functional variables.

iii) Identify the failure modes to that affect the system and the noise variables excite the failure modes and reduce the system performance;

iv) Summarize the identified system critical parameters and variables that affect this system;

v) Define the operating window of the selected factor by identifying the range that keeps the failure modes constant;

vi) Adjust the system control variables to maximize the operating window range.

vii) Analyze the trade-off between time and level of robustness wanted in order to repeat the cycle.

An adaptation of the steps will be used to fit the purpose of the research. In this study, the operating window is not meant to be maximized, nor is a nominal set point to be defined. The research aim, is simply to identify the operating window from a variety of possible design configurations in order to prove the hypothesis that tight performance variations would lead to a large operating window and vice versa. This will be necessary because of the resources constraints that are present in the target application and the available stencils that had been developed for a pervious experiment. In order to adapt the methodology proposed by Clausing and Fey (2004), a flowchart was developed and is presented in Figure 2.

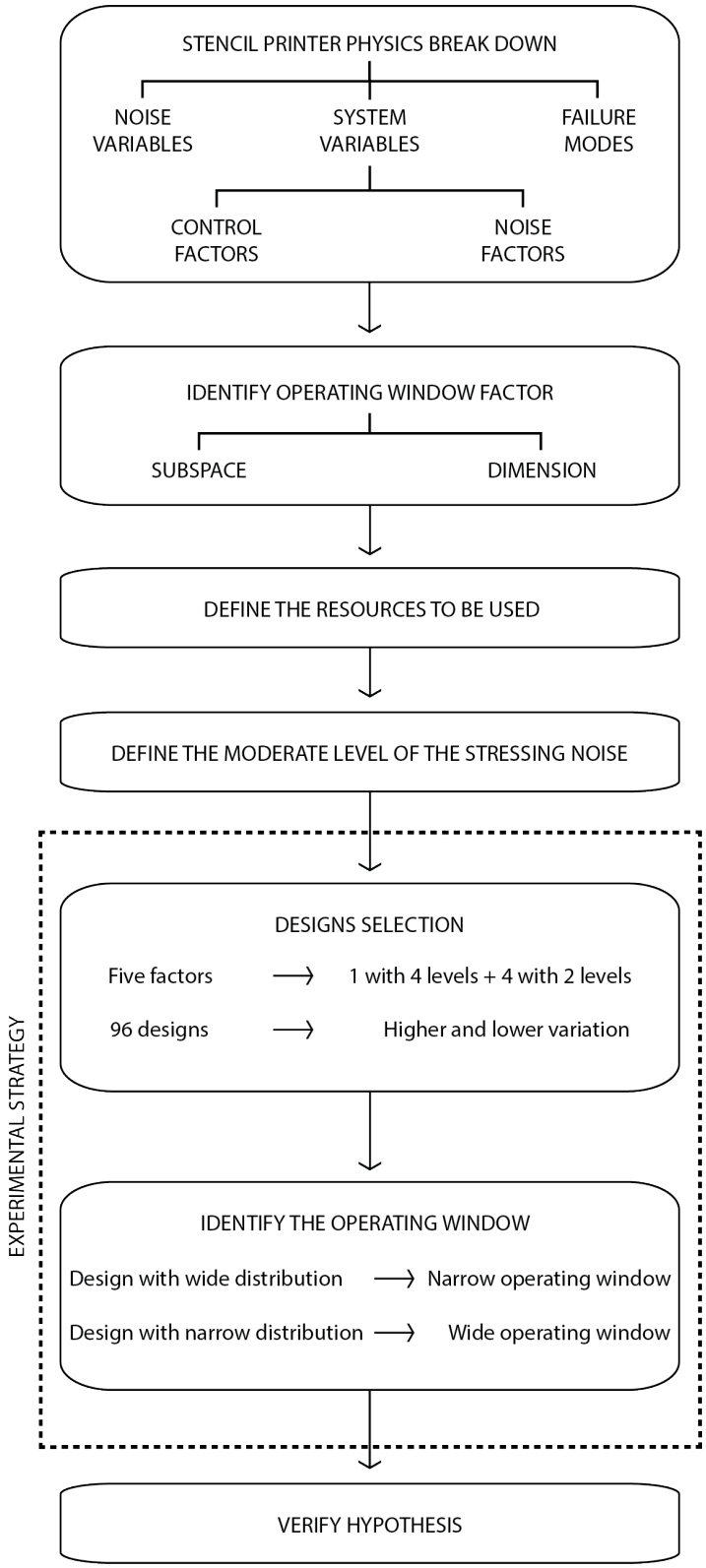

Figure 2. Methodology flowchart. This figure illustrates the steps of the research methodology.

The methodology will start with an analysis of the system physics to identify the critical parameters that compose this system. The operating widow factor and the noise factors to be used will be identified based on the previous analysis. All the equipment, tools, and supplies will be selected to represent the system functions. With all system factors identified, an experiment will be carried out to test the performance of all available designs. Two designs with opposed performance results will be selected and the operating window will be developed for each one of them. Finally, an analysis of both operating window will be performed to identify the predicted difference between these designs.

Materials

Stencil Printer.

Machine specification. A stencil printer is part of the surface mount technology (SMT) necessary to manufacture printed circuit boards (PCB). Surface mount technology allows the production of smaller, lighter, faster and cheaper PCBs. The stencil printer applies solder paste to the PCB where the components will be placed (Omori & Miller, 1992). The solder paste is a mixture of solder particles with flux. The solder particles are required to form solder joints while the flux gives the flow characteristics of the paste and is the means by which the solder particles are held together. A stencil is a metal plate with small holes (apertures) arranged in a pattern that mirrors a specific layout for each PCB that will be processed through the stencil printer machine. The apertures match each PCB spot (pads), where the solder paste will be applied. The solder paste is spread over the stencil by a squeegee. The squeegee is a blade that runs over the stencil during the printing process and pushes the solder paste into the stencil apertures (Prasad, 1997). Figure 3 shows an image of the machine, the stencil and the squeegee blade as described. The machine used in the experiment is the MPM Momentum (see Appendix B).

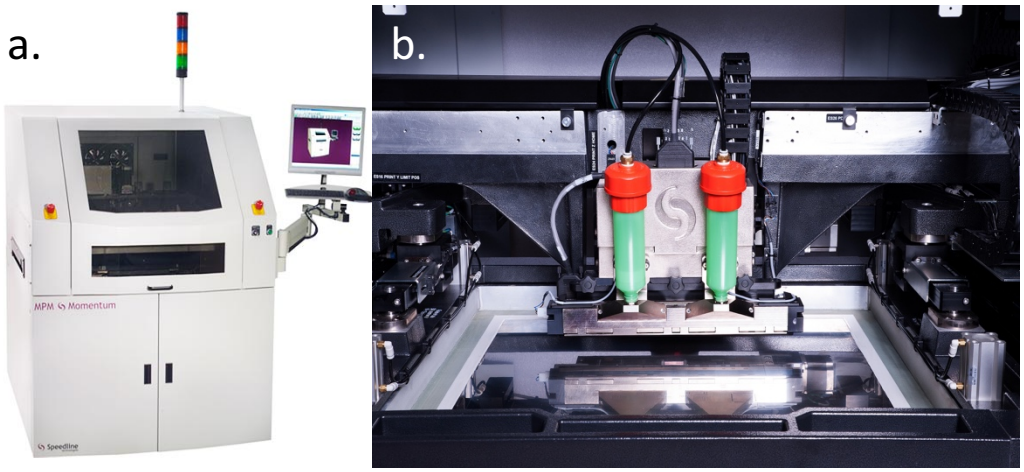

Figure 3. Stencil printer. This figure is a picture of the Stencil printer (a) and its parts (b). Retrieved June 28, 2016 from http://www.speedlinetech.com. Copyright 2016 by the Illinois Tool Works.

Operation. The process of applying a uniform quantity of solder paste to the PCB pads is automatically done by the stencil printer after the control parameters are set. The setup involves introducing and aligning the stencil that matches the PCB configuration, applying the variables' set points on the machine computer and applying the proper quantity of solder paste over the stencil. After the setup is done, the process starts and with the squeegee operation, the machine spread the solder paste that penetrates the apertures and settles on the PCB pads. Figure 4 shows a detailed flowchart of the process. While the black box diagram in Figure 5 represents the system inputs and outputs.

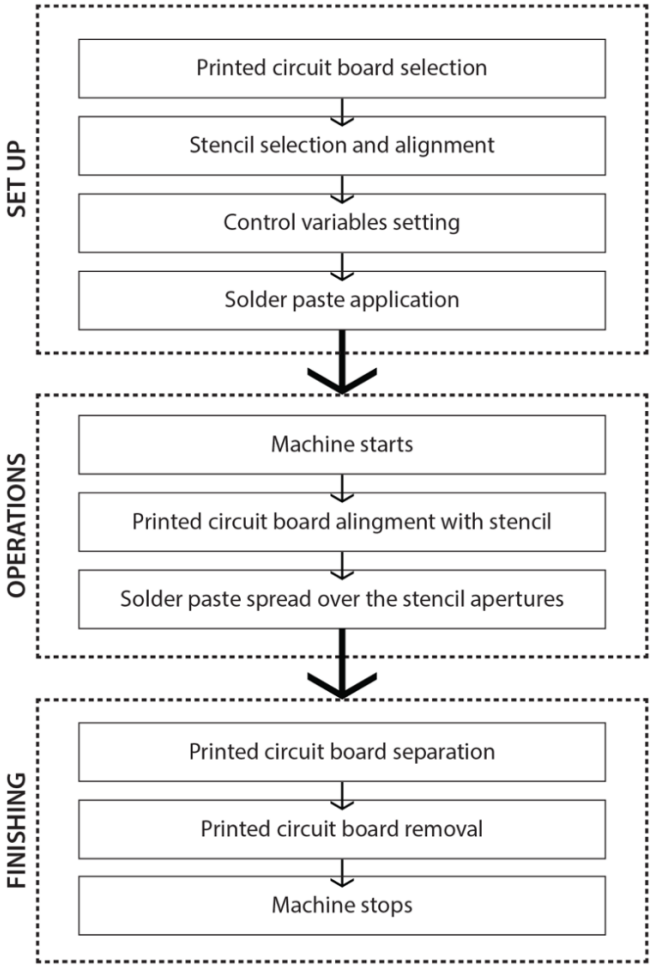

Figure 4. Stencil printer flowchart. This figure illustrated the steps of the stencil printer production process.

A detailed printing process is shown in Figure 6. When the machine starts, the wafer aligns with the stencil in a way that each pad match with the aperture on the stencil. After the alignment, the wafer gets close to the stencil until the defined print gap. After the board is in position, on step 1, the Squeegee starts rolling the solder paste. The apertures are filled with solder paste that is pushed by the squeegee. On step 2, the board is detached from the stencil. The solder paste that filled the apertures is transferred to the pads and the print is finished.

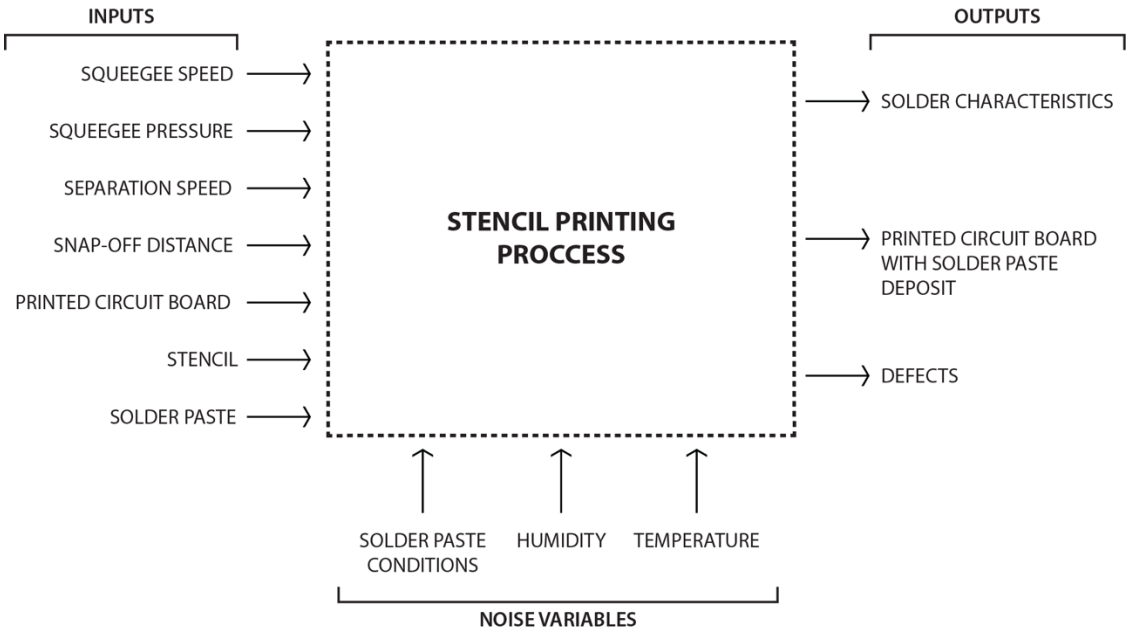

Figure 5. Stencil printer diagram. This figure illustrates the process inputs and outputs.

Motivation. The SMT assembly process is composed of Stencil printing, Component placement, and Reflow soldering. Although the three processes have their own respective operating difficulties, the solder paste printing process is responsible for 63.8% of the SMT assembly defects (Mangin, 1991). In order to effectively reduce the defects on PCBs, the stencil printing was selected. The design of a process that accounts for the failure modes and noise effects is an alternative to minimize the defect rate of the SMT assembly instead of using the traditional approach of solving problems repeatedly (Hoyle, 2005).

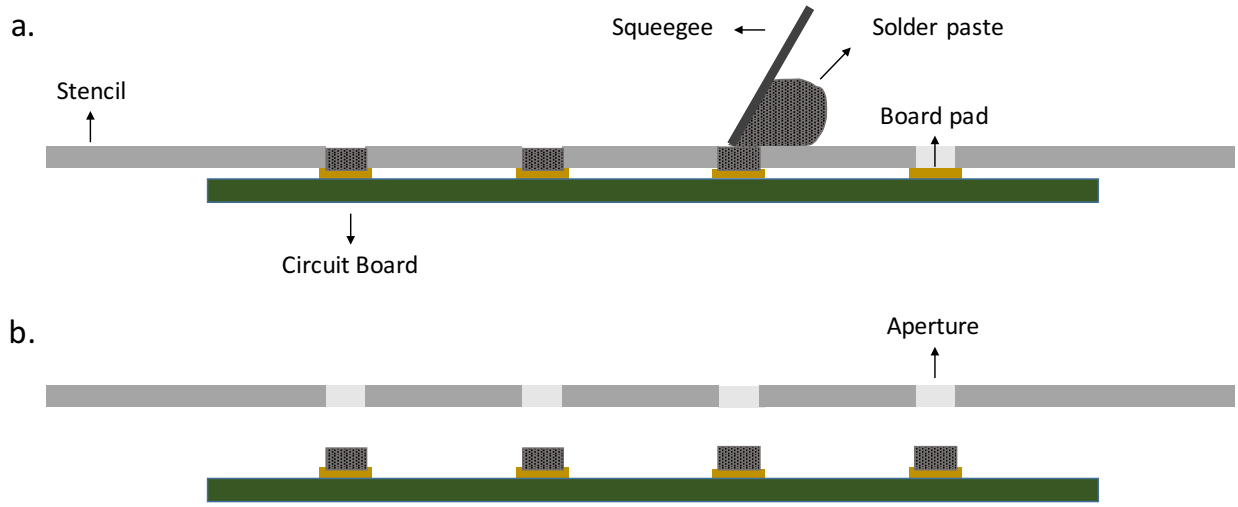

Figure 6. Solder paste printing process. This figure illustrates the detailed steps of the stencil printing process, with the squeegee pushing the solder paste (a) and the stencil separation (b).

Failures. The failures will be identified by the application of a Fault Tree Analysis (FTA). The FTA gives a visual representation of the failure events and their consequences, making it easier to identify these failures and to mitigate them during the system design phase (Shu, Cheng, & Chang, 2006).

Physics Breakdown. A deep understanding of the system physics has significant importance to the application of the operating window methodology. To develop this knowledge, the project starts by breaking down the system structure. The objective is to understand the relationship between the system variables, failure modes, and noise variables. The system structure is shown in Figure 7. It can be seen that several factors can influence the printing process. However, for the basis of this study, several of these factors will be kept constant throughout the study.

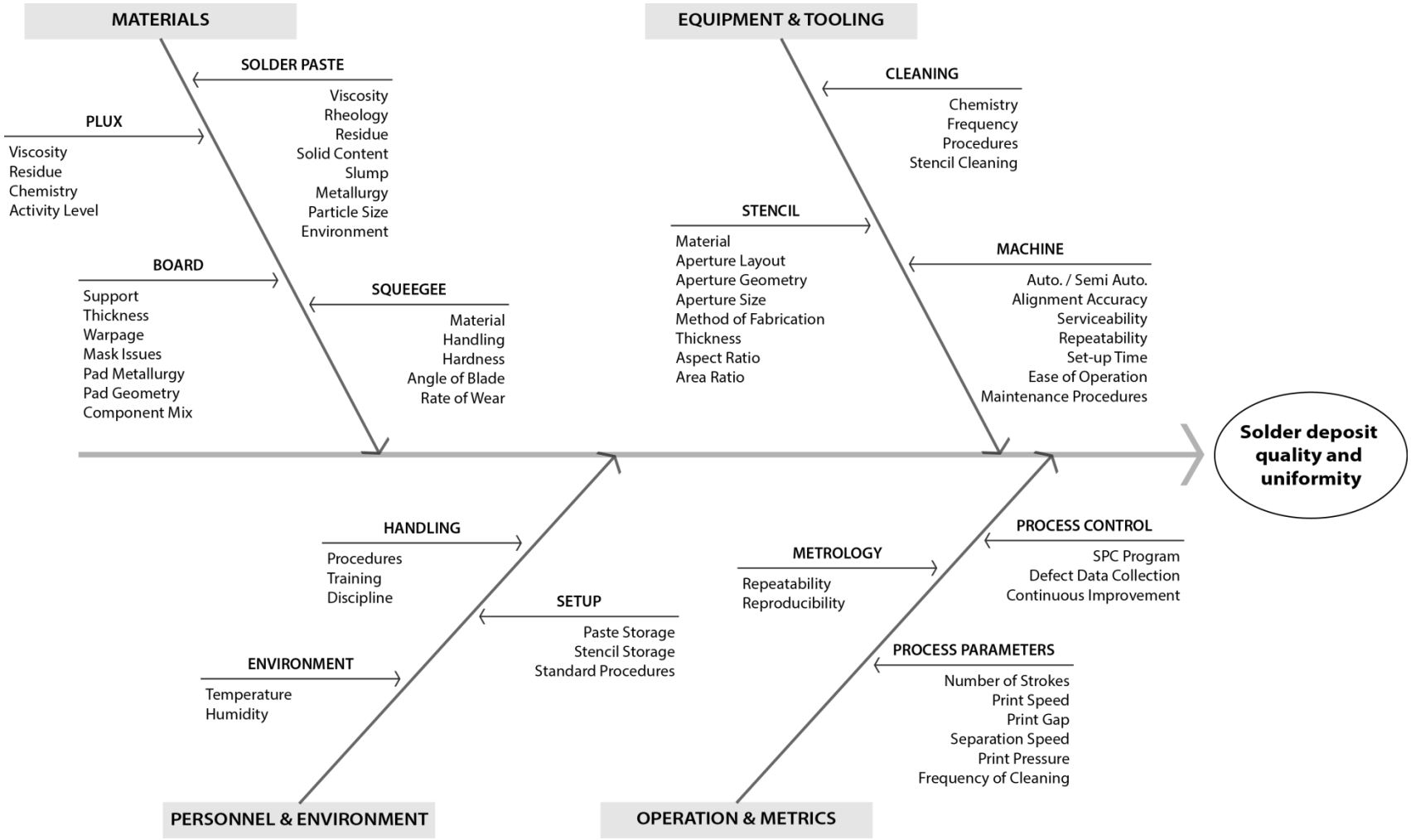

Figure 7. Stencil printer variables. This figure illustrated the variables related to the stencil printer activity. Adapted from "Surface mount technology" by Prasad, R. P., 1997. 2th edition. Copyright 1997 by Chapman & Hall.

Measurement. The system output will be considered the Transfer Efficiency (TE) of solder paste from the stencils' apertures. Amalu et al. (2011) states that the understanding of the TE is vital for the stencil printing process. This measurement is a ratio of the volume of solder paste deposited over the PCB to the aperture volume. Ideally this ratio should be 100%. A 100% Transfer Efficiency means that all solder paste that filled the aperture was transferred to the PCB. Therefore, the apertures and solder paste volumes will be measured.

Aperture measurements. Aperture volumes are easily calculated from the stencil manufacturing drawings. However, these values are nominal values and do not reflect the actual values of each aperture as the manufacturing process is susceptible to variations. A good practice is to design apertures on the corner of the stencil where it can be cut and measured with precision. This would enable the use of aperture real dimensions and would enable a better future replication. For the purpose of this project, this step will not be possible as the stencils are already built and the data in the previous study is not available. However, an alternative will be used. The actual aperture sizes from each stencil made with the Electroform and the Laser technologies will be measured.

In order to measure the volume of each aperture, a SmartScope Quest 650 (shown in Figure 8) from the Optical Gaging Products, Inc. (OGP) facility was used. The machine uses optical sensors, a laser beam, and a touch probe to measure parts. The machine specifications are shown in Appendix C. The machine is operated by Zone3 software. The software allows a program to be written to measure parts features based on a computer-aided drafting (CAD) model. In addition, the same program can be used to make measurements on other identical parts. After the program is written all the measurements are made automatically on the CAD features selected.

Figure 8. SmartScope Quest 650. This figure illustrates the SmartScope Quest 650 machine. Retrieved June 28, 2016 from https://www.ogpnet.com/north-america/systems/video-multisensor/smartscope-quest/smartscope-quest-650/index. Copyright 2015 by Quality Vision International, Inc.

Solder paste inspection. The solder paste deposit on the printed board was measured using a Koh Young KY-3020T (see Figure 9). The machine is a bench-top metrology device and its specifications are shown in Appendix D. The machine operates by emitting light from different sources at predetermined angles onto a target. The lights generate a grid format and are applied a predetermined number of times over a path. Pictures are obtained from this illuminated path. The equipment is then able to measure the patterns on the images and calculate the target tridimensional surface (Hur, Jeon, Kim, Yun, & Hong, 2014).

Figure 9. Koh Young KY-3020T. This figure illustrates the Koh Young KY-3020T. Retrieved June 28, 2016 from http://kohyoung.com/en/ky-3020t/. Copyright 2008 by Koh Young Technology Inc.

To measure the solder deposit on the board, a drawing of the apertures is needed. The machine generates the program based on the drawing and on the selected pads to be measured. In order to reference the machine, the fiducials are used and several bare board are measured to identify their pattern. With the program created the machine automatically measure the volume of solder paste deposited on the PCB.

Operating Window Methodology

Identifying the operating window factor. The identification of the critical functional variables is the first step in the development of robustness. To identify these variables it is necessary to understand the system physics. With the understanding of the part interactions, it is possible to identify the critical variables. This process is facilitated by the use of reliability tools (Clausing & Fey, 2004).

Based on the previous step of the methodology an analysis of the system functions and failure modes will help to identify the operating window factor. Considering the stencil printer

physics, it can be noted that several opposing failure modes are present. Failures can occur when a small amount of solder paste is deposited on the pad. On the other hand, the excess of solder paste can cause a different type of failure. These failures can be induced by variation in the squeegee pressure and these failure boundaries can be defined by low and high pressure values, respectively. At the lower level, the lack of pressure can result in not enough solder paste being applied to the pad. On the other side, high-pressure levels can cause an increased amount of solder paste to be deposited generating, for example, slumping, bridging, and scooping phenomena. The squeegee pressure is considered as a strong operating window factor candidate for this study.

Failure rate and noise level. Joseph and Wu (2004) identified that the main concept behind the effectiveness of the Operating Window Methodology is the enlargement of the failure probabilities. The method of failure excitation reduces the sample size necessary to estimate the factors effects (Joseph & Wu, 2004) and it speeds up the learning cycles. As one of the objectives during development is to identify when the system fails, the increased failure frequency reduces the number of runs of the experimental strategy. Joseph and Wu (2004) highlight the necessity to spend some effort to find a 50% failure probability known as the half of the Lethal Dose (LD50). However, Clausing (2004) states that the exact percentage might not be necessary, as long as the failure modes are significantly amplified. The LD50 value is also questioned by Leitnaker and Mee (2004).

In this research the aim will be to amplify the failure rate but quantifying the failure rate or getting to an exact fail rate number will not be a focus. In order to excite this failure occurrence, a noise factor has to be linked to particular failure mode and fixed at a moderated

level. The objective is simply to reduce the number of samples necessary to find the operating window.

Experimental plan

Before starting experiments, it is recommended to validate that the measuring system is adequate as they have great impact on the identification of a product quality (Pan, 2006). This will be done through a Gage Repeatability and Reproducibility (Gage R&R). This analysis will identify if there is significant variability in the measuring system. Pan (2006), showed that the level of variability due to the measurement system should be less than 10% specification width. So, it will be possible to rely on the measurement system, if the variability due to Koh-Young measurements is less than 10% of specification width.

The process of selecting two designs and identifying the operating window for both require data collection. These data will be collected with two different experiments. First is necessary to identify the distribution for each available design and to look at the effect of these different design variables. This will be done through a full factorial design under normal operating conditions. Secondly, in order to test the hypothesis of this thesis, the experiment is performed to identify the operating window for two of the available designs. The OW will be applied to the extreme cases to see if the variability and the operating window are indeed correlated. This is done by a sequential trial and error approach under high fail rate operating conditions.

Designs selection. The first experiment will serve as a pre-testing for the operating window experimental strategy. It aims to identify designs with different distributions associated with changes in the stencil design parameters. To assess a significant difference, the design with the smallest variation and the one that has the largest variation will be selected. A full factorial

experimental design is necessary to assess the distribution of each available design. As a standard Robust Design approach, all the control parameters are fixed at a nominal value. All the designs will be analyzed under the same printing conditions. This nominal level for each control parameter is defined based on expertise and industry accepted standards. For each run, a transfer efficiency distribution is plotted. The concept of the operation window is to be tested by identifying the operating window for the factor's levels from the two selected designs.

For the Stencil printer experimental design, five factors are to be evaluated as is shown on Table 2. The apertures were manufactured with Laser, laser with nano-coat, electroformed with nano-coat, and electroformed with nano-coat polished. For each stencil, there are also two different thickness designs which are four and five mils. In addition, there are different aperture designs for the type of component selected. It was selected the components with dimensions of 0.1"x0.05" (01005). The apertures for this component were manufactured in square, rounded corner, and bow tie shapes. Moreover, there are apertures with different dimensions, 9x9 mils, and 8x10 mils. The same solder paste was used in each experiment.

Table 2

Design factors and their levels.

Factors	Stencil Manufacturing Type	Stencil Thickness	Aperture Design	Aperture Size	Aperture Orientation
Levels	Electroformed with nano-coating	4 mils	Rounded corners	9x9 mils	Horizontal
	Electroformed with nano-coating polished	5 mils	Sharp corners	10x8 mils	Vertical
	Laser		Trapezoid		
	Laser with nano-coating				

Given the number of factors and their levels it would be needed 96 runs to assess all factors combinations. For this reason, it would be reasonable to think in reducing the number of runs, necessary to analyze all the factors, with a Taguchi Orthogonal array. However, to test the hypothesis without any aliasing, we chose to run the full factorial design. Moreover, on a product development effort, we want to test all the alternatives. Even though it could be possible to reduce the number of runs, this is not a constraint for this experiment. In addition, because of the board design, we will have four replicates at each run.

This experimental part of the present research is a replication of the study by Mohanty et al. (2011). The same stencils and machinery were used. The only difference would be the use of a different solder paste manufacturer. However, setting the stencil printer for the same parameters as in Mohanty et al. (2011), it was noticed that the squeegee was not pushing all

solder paste and an excess of solder paste was left over the stencil after the print (Figure 10). This problem shows that the solder paste is not rolling smoothly and probably not filling the apertures. The cause of this problem was assigned to the different solder paste used. Although the same type was used, different properties can be found between manufacturers. The solder paste property has a great impact on the printing quality (Prasad, 1997). The material viscosity and its variations during the printing process are determinant factors for the entire SMT mounting process. The incorrect storage and pre-production procedures can also change the desired properties. The type of solder paste is based on the solder particles size. The types vary from Type-1 to Type-6. The specification type for the PCB to be used is the Type-4 (Prasad, 1997).

Hence, the printing pressure was adjusted until a good flow of solder paste was found (Figure 10). The pressure was changed from 16 to 22 pounds (lbs.). With these changes, the standard setting to be used is as follow:

- Solder Paste – Loctite Type IV, lead-free paste
- Squeegee speed – 1 in. per second
- Squeegee pressure – 24 lbs.
- Separation distance – zero print gap
- Separation speed – 0.9843 in. per second
- Cleaning frequency – dry wipe after each print with vacuum suction
- Print direction – both rear-to-front and front-to-rear
- Number of prints – one replication after the third print
- Replication per design – 96 pads per design

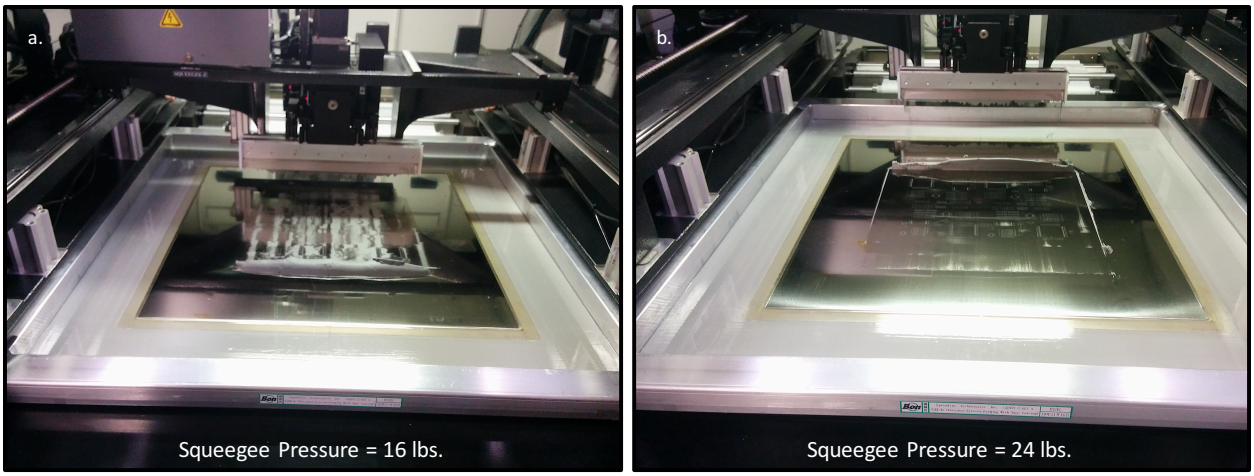

Figure 10. Printing flow. This figure illustrates a print where solder past stayed on the stencil after the print (a) and a clean print (b).

The nominal design setting was based on the results of Mohanty et al. (2011). Their results show that electroforming with nano-coating stencil has a greater process capability for all the apertures. Mohanty et al. (2011) also conclude that the aperture Area Ratio (AR) is directly correlated with the transfer efficiency increase and variance decrease. That being said, the aperture with greater AR is a 9x9 mils aperture with rounded corners on a four mils thick stencil. Moreover, they also conclude that there is no significant difference due to the apertures orientation. The vertical orientation was selected as it presents a larger space between the apertures during the print.

Constraints. Different noise factors affect the lower and upper thresholds. The lack of solder deposited is hampered by solder paste with high particle size or a poor aperture finish. One example is the finish allowed by the Laser technology compared to an Electroforming with nano-coating polish. On the other side, a high stencil thickness or a high print gap should generate a higher deposit of solder paste. But most of these factors are design parameters or were already mitigated with the development of the stencil printing technology.

In addition, physical design variables are harder to change and the operating window is applied to its manufacturing process. On the stencil printer, the aperture sizes are one example. The operating window methodology can be applied to the development of the stencil but its application on the printing process will not enable changes to the apertures as the stencil is already built. The manufacturing of a stencil is an expensive task and it is not readily available for this research. For these reasons, the analysis of the aperture sizes is restricted to a set of available stencils, selected to develop the experiment.

Identify the operating window. Experiments are developed to validate hypothesis and theories about how a system works. They require the definition of the problem, the selection of response, the identification of factors and factor levels, the design and execution of the experiment, data analysis, and conclusions based on the analysis result (Montgomery, 2013).

The second experimental step will follow a trial and error approach. Although this approach is criticized by many authors (Box, Hunter, & Hunter, 2005; Czitrom, 1999; Logothetis & Wynn, 1994; Wu & Hamada, 2009), a sequential design will be used. It should be noted that the trial and error method in the Operating Window methodology is not random. Rather it is guided by the insights generated by failure. The trial and error sequence is similar to the one used by Joseph and Wu (2002) to find the thresholds on their experiment. However, no equations will be applied, instead, a more intuitive approach will be used. Sequential designs, in comparison with a single experimental design, are preferred to identify how changes in the design parameters affect the system performance in the design phase (Frey & Jugulum, 2006). Some authors advocate the adaptation of experimental plan based on the data result (Daniel, 1973; Friedman & Savage, 1947; McDaniel & Ankenman, 2000; Qu & Wu, 2005). This allows the experimenter to learn during the experimentation and combine this learning process with his

knowledge of the system, to identify key points of the system design. In the Operating Window methodology this learning is speeded up by the high failure rated applied as the insights are generated by the failures.

To define the system's operating window, at the first time, it is necessary to set the system to its best operating condition. On a development process, the setting would be defined based on previous experience with a similar process. The second step is to input the fixed noise variable and adjust the operating window variable to have a high failure rate. A stressing noise level is set at a moderate level and its level is increased each time the operating window is improved (Clausing, 2004).

For the upper threshold, Mohanty et al. (2011) applied a transfer efficiency limit of 140%. This was the value defined as a short circuit failure. Although for the lower limit, Mohanty et al. (2011) applied a transfer efficiency limit of 60%, Anselm (personal communication, June 3, 2016) claimed that in certain cases it is possible to have a good solder joint with transfer efficiency as low as 30%. A minimum print deposit was estimated for the 01005 components using the methodology applied by Schake and Whitmore (2016) for 008004 components. The minimum paste deposit is two times the minimum solder joint volume (Equation 2) as the flux from the solder past occupy 50% (on average) of the total deposit volume. The minimum joint volume is the sum of the solder joint volume from the sides of the terminations (V_1 and V_2) (Equation 3), from the end of the termination (V_3) (Equation 4) and from the solder joint under the termination (V_4) (Equation 5) as can be seen in Figure 11. However, differently from what was used by Schake and Whitmore (2016), instead of just the solder thickness (G) the joint volumes will be calculated using a triangle approximation as was used by Schake and Whitmore (2016) to calculate Y, but not to calculate the volumes.

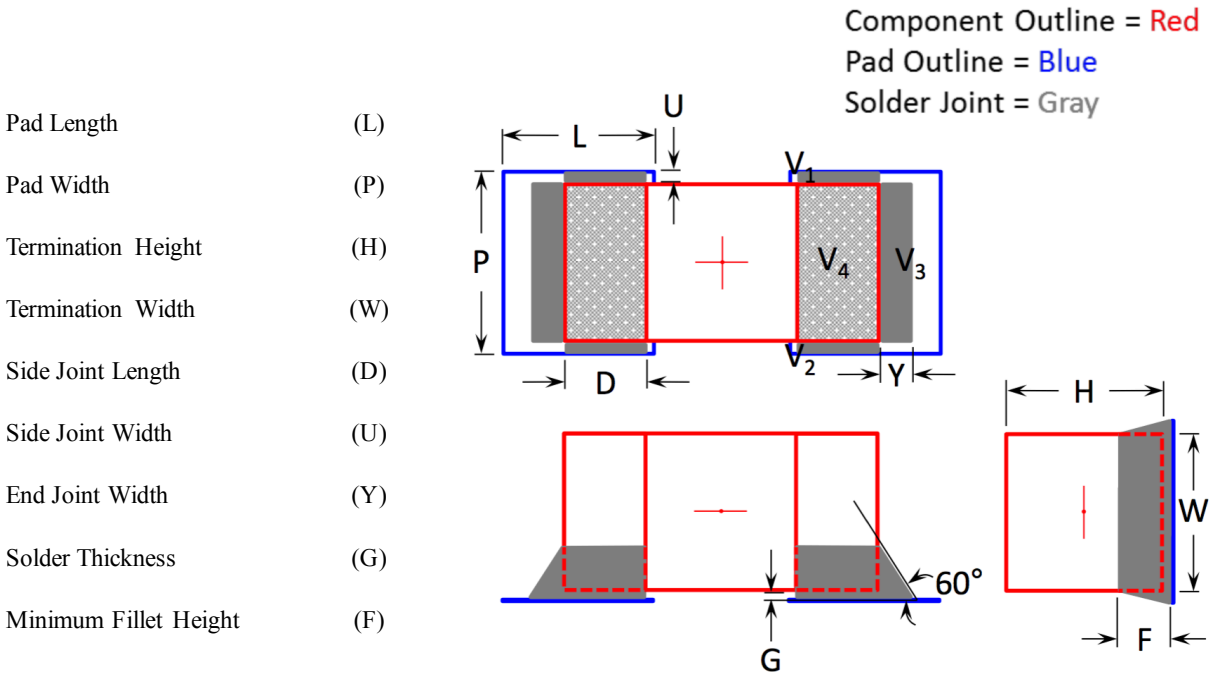

Figure 11. Minimum print deposit volume estimation. This figure illustrates the dimensions used to estimate the minimum print deposit volume. Adapted from " First Look at Printing Metric 0201's " by Schake, J., & Whitmore, M., 2016. *International Conference on Soldering and Reliability Conference*. Copyright 2016 by the Surface Mount Technology Association.

$$V_{min} = 2(V_1 + V_2 + V_3 + V_4) \quad (2)$$

$$V_1 = V_2 = D * U * (\frac{F}{2}) \quad (3)$$

$$V_3 = Y * W * (\frac{F}{2}) \quad (4)$$

$$V_4 = D * W * G \quad (5)$$

Robustness Developing Cycle

Noise level increase. The next step of the methodology would be to increase the level of the noise factor, repeating the activities to identify a more robust operating window. When the noise level is changed, the previous operating window will be reduced to the new operating condition. Efforts are needed to expand the operating window again. The new operating window would make the system robustness increase for the new condition and for the previous noise level condition as well (Clausing, 2004). This phenomenon can be seen in Figure 12, where the operating window for a high noise level increases when the level of noise reduces.

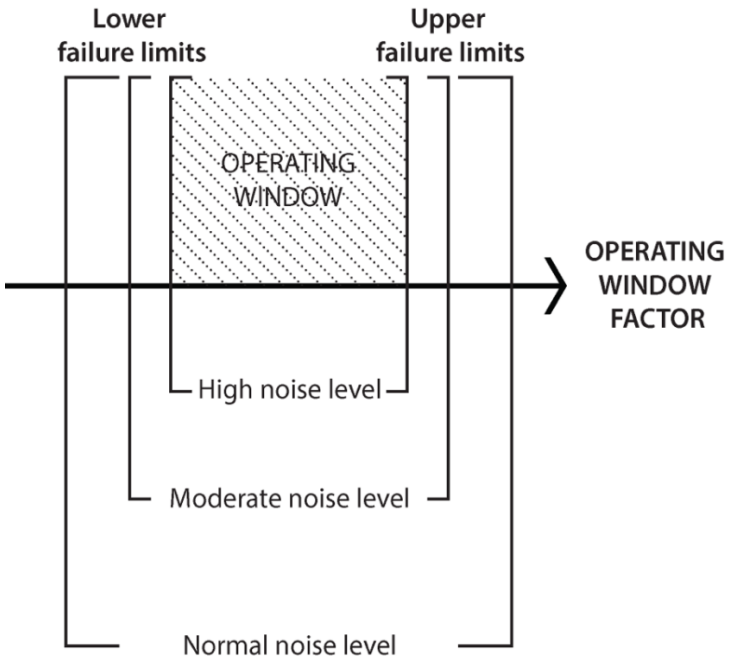

Figure 12. Progressive development. This figure illustrated the effect of noise on the operating window. Adapted from "Operating window: An engineering measure for robustness" by Clausing, D. P., 2004. *Technometrics*, 46(1), 27. Copyright 2004 by the American Statistical Association and American Society for Quality.

For the stencil printer example, gradual changes in the squeegee pressure would reflect the noise level increase. At each noise level, a new operating window would be identified. The operating window of the last noise level used would be the final system adjustment. However, this step was not developed in this paper.

Robustness and time trade-off. Robustness has to be gradually developed into a system. At the initial developing cycle, the system presents very weak robustness and is vulnerable to large operating variations. If a significantly high noise level is applied without any robustness is previously build into the system, the system will fail to be functional (Clausing, 2004). This situation explains the necessity of increase the noise level at each developing step as is proposed.

Although the noise level growth increases the system robustness, the developing time is a constraint of new product developing cycle. Usually, this constraint is related to the product time to market (Clausing & Fey, 2004). If too much effort is applied to increase the system robustness, the system might not be ready in time to be produced. This trade-off define how much robustness will be developed and that further development will need to be postponed to the next system generation.

There is not an optimal quantity of interactions to develop the system robustness to the desired level. This will depend on the system complexity and the project intention (Clausing & Fey, 2004). Because of the objective of this research just one interaction will be performed to develop the system robustness on the stencil printer example.

Analysis and Results

This section will present the analysis proposed on the methodology and the results obtained from it. First, to deal with the constraint exposed, a measurement of the apertures is made. Secondly an analysis of the system physics is developed through the application of a FTA. The identification of the system's critical parameters, noise factors and failure modes is made based on this analysis and on previous experience with the system. Next, the results of the first experiment performed are shown. This section ends with the application of the operating window methodology on the two selected designs.

System Physics

From the FTA that was developed (see Appendix A), the main failure modes that were identified were tombstoning, open circuits, short circuits, and missing components. From the analysis, the effect of each main parameter can be seen with respect to how it can lead to failure event generation, as can the strong relation that failures have with the solder volume deposited.

The most significant failure modes for this research are identified as open circuits when the solder joint is not sufficient to connect the board pad with the component and short circuits when the solder joint of one pad connects with a solder joint from other pad. However, they are not directly assessed by the experiment. The amount of solder paste deposited will only give an idea of the solder joint. To fully identify the failure modes, the entire soldering process should be completed. To deal with this constraint, limits were defined to assess the recommended amount of solder paste that would give a good joint.

From the FTA analysis, it was concluded that squeegee speed, squeegee pressure, and the separation speed play a greater role on stencil printing process control variables. These variables have a significant impact on the quantity of solder paste transferred to the PCB pads. High

separation speed causes the solder paste release process to be difficult, which results in a low quantity of solder deposited over the pad. A low separation speed results in a higher quantity of deposited solder paste but can cause problems with the printing quality. High printing speed can also cause a lack of solder paste deposit due to the reduced period of time to fill the aperture with solder paste. Low printing speed maximizes the time to fill the aperture but can cause problems on the shape of the deposit.

Operating Window Factor

This study applied the operating window in terms of the squeegee pressure, as is one of the most significant factors to access the desired print volume. The squeegee speed was used as the noise factor. Two levels of squeegee speed are fixed to be applied as a noise factor, one level for the lower threshold and the other for the upper threshold. The separation speed is kept constant the entire experiment. One could note that the three factors could be used to access a three-dimensional operating window, but this is not the purpose of this study and will be considered as a possibility for future work.

Resources Definition

In order to measure the transfer efficiency, the aperture volume need to be assessed. Several apertures were measured using an optical metrology machine. The OGP Quest 650 enabled a precise measurement on a large part. The measurements were taken on 01005 apertures of Laser and Electroforming with nano-coating stencils to represent the technology variation. The average of the aperture sizes (Table 3) was applied for the calculation of the transfer efficiency.

Table 3

Aperture Size.

Nominal Sides Length	Measured Sides Length (mils)	
	Electroforming	Laser
10 mils	9.51	9.60
8 mils	7.57	7.56
9 mils	8.67	8.80

Although the Koh Young equipment are well established in the industry and the quality of its measurement are well known, a Gage R&R study statistically validate the specific machine installed on the Center for Electronics Manufacturing and Assembly (CEMA). For this purpose, one printed board was submitted to the measuring system three times. The board was printed using a four mils stencil, electroformed with nano-coating and polished, on a pre-experimental test.

Based on the Gage R&R study, it is possible to conclude that the measuring system is adequate. The Koh Young repeatability accounts for only 0.01% of the overall variability (see Table 4). There is no reproducibility as the same machine was used. In addition, the measuring system is responsible for only 0.85% of the specification width (see Table 5). Since the percentage due to parts is greater than 70%, it is possible to rely on the Koh Young measurements. From the histogram on Figure 13, it can be seen that the part to part variations contributes to almost all system variability.

Table 4

Gage R&R variance components.

Source	VarComp	%Contribution (of VarComp)
Total Gage R&R	7.60E+07	0.01
Repeatability	7.60E+07	0.01
Part-To-Part	1.05E+12	99.99
Total Variation	1.05E+12	100.00

Table 5

Gage R&R process variations.

Source	StdDev (SD)	Study Var (6 × SD)	%Study Var (%SV)
Total Gage R&R	8715	52291	0.85
Repeatability	8715	52291	0.85
Part-To-Part	1025194	6151162	100.00
Total Variation	1025231	6151385	100.00

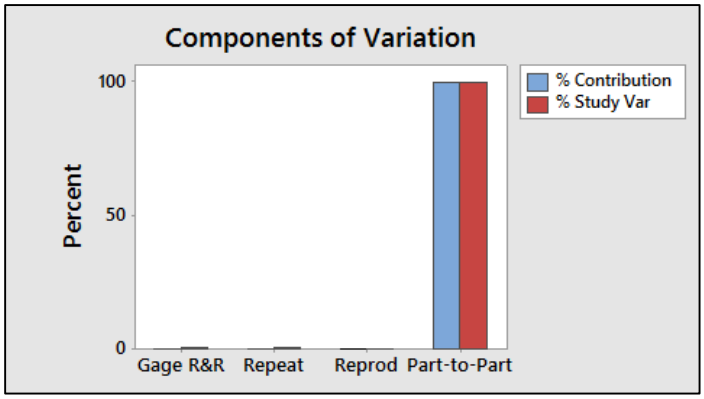

Figure 13. Gage R&R components. This figure illustrates the components of the measurement variation.

Noise Level

On the stencil printer experiment, the squeegee speed and cleaning strategy were applied as noise factors. The squeegee speed has opposed effects on the printing process and is applied to both thresholds. The cleaning strategy has a significant impact on the amount of solder paste deposited. On an industry basis, a higher speed could increase the productivity and the cleaning strategy could also increase productivity and reduce production costs. The squeegee speed was set to 3 inches (in.) per second but changed later to 2 in. per second for lower threshold and set to 0.5 in. per second for the upper threshold. The cleaning strategy was kept at every run for the lower boundary and no cleaning was set for the upper boundary.

The squeegee pressure is defined as production noise. Moreover, a one-dimensional operating window is stated. Only one variable in the system-variable space with two opposing failure modes will be used to identify the system's operating window.

Design Selection

Experiment. The full factorial design was run on the same day, with the same conditions. Two dummies prints were performed before each valid print for each stencil in order to get the machine adjusted with the settings after the changeover. The measurements on the valid printed boards were taken right after the print on the Koh Young machine. A summary of the obtained results is available in Appendix E.

The analysis started by organizing and plotting the data on boxplots charts. On Figure 14, it seems that there is not a significant difference between the apertures sizes and its orientation. However, the four mils stencil seems to result in a greater transfer efficiency than the five mils stencil. In addition, the trapezoid designs result in a smaller transfer efficiency as compared to the other designs but it also has a smaller amount of variation. All of the

manufacturing types for each stencil results in a large amount of variation making hard to make any conclusions with respect to this factor.

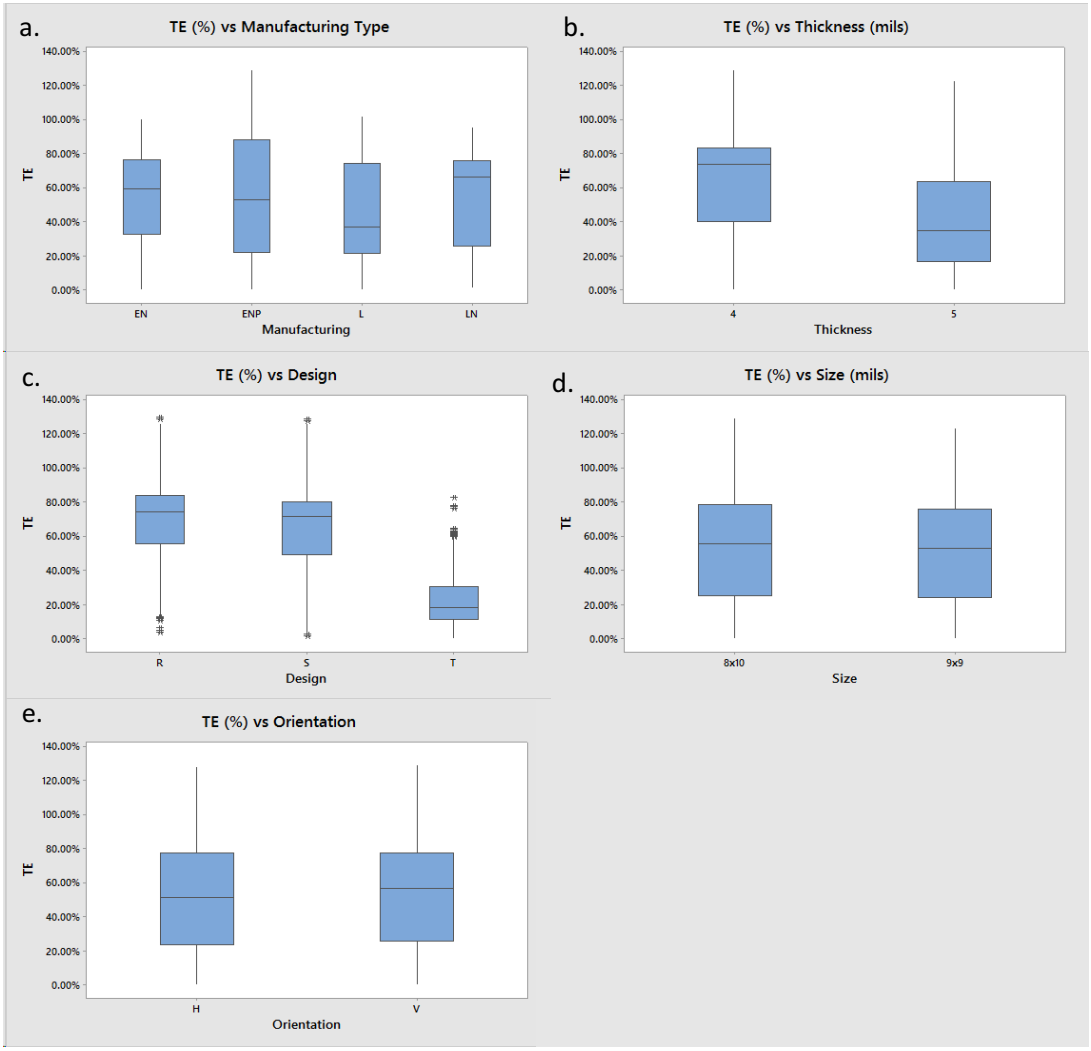

Figure 14. Boxplots diagram of main factors. This figure illustrates boxplots diagrams from stencil manufacturing types (a), stencil thickness (b), aperture design (c), aperture size (d), and aperture orientation (e).

The results were separated on Figure 15 to have a better perspective of the data. It can be seen that the different apertures sizes seem to have the same distribution. The same can be noted from the apertures orientation, but a difference in the variance seems to be present. Moreover, the trapezoid design presents the lowest mean for both apertures sizes. Looking at the results

based on the stencils, it can be seen that the four mils stencil appear to have a better performance than the 5 mils. On the 4 mils stencil, the electroforming with nano-coating polished stencil presents the highest mean but a high variation and the electroforming with nano-coating present the smallest variation. But on overall the Laser on the five mils stencil have the smallest variation and lowest mean.

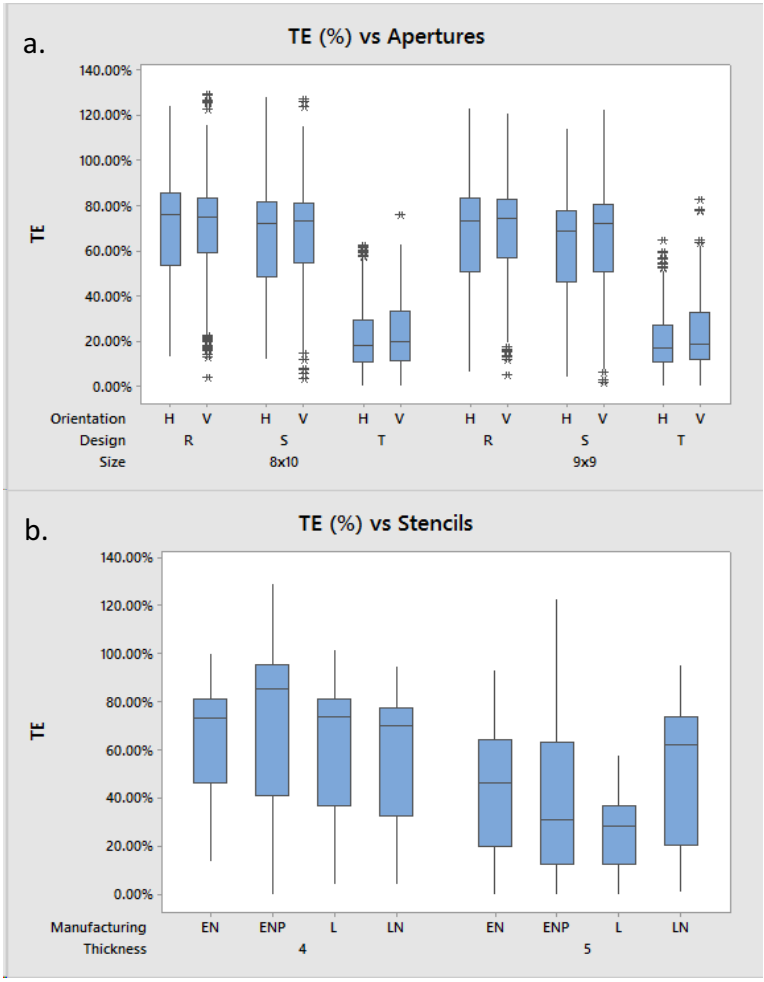

Figure 15. Boxplot diagrams with factors levels. This figure illustrates boxplots diagrams divided by aperture factors level (a) and by stencil factors level (b).

Considering this preliminary analysis, it can be noticed that some designs with small mean will present small variation as in the case of the trapezoid aperture shape. This seems to be related to proximity to the bottom limit of 0%. Because of this possibility, a lower limit will be

applied to the results. The limit will be calculated based on Schake and Whitmore (2016) equations.

Two minimum volumes are necessary as two aperture sizes are being analyzed. The minimum volume calculated for the 9x9 apertures is 1.43 nanoliters (nl) and for the 10x8 apertures is 1.63 nl. Table 6 shows the values used on Schake and Whitmore (2016) equations to calculate the minimum volume for the 01005 apertures. Hence, the designs that resulted in mean volumes lower than these values were eliminated from the analysis. This action eliminated 30 out of 96 possible designs.

Table 6

Minimum solder calculated values.

Component		1005	
Pad Size		10x8	9x9
Pad Length	L	203.2	228.6
Pad Width	P	254	228.6
Termination Height	H	200	200
Termination Width	W	200	200
Side Joint Length	D	120	120
Side Joint Width	U	27	14.3
End Joint Width	Y	37.5	37.5
Solder Thickness	G	15	15
Minimum Fillet Height	F	65	65

The remaining 66 designs had their distribution plotted and analyzed individually to identify the ones with the lowest and highest variations. The final choice was made based on their standard deviation. Figure 16 shows the distribution of the two designs selected. It can be seen in the figure, both designs mean and standard deviation. In addition, it is shown how the distribution is centralized in relation to the limits specified on Mohanty et al. (2011). The specifications of the designs selected are shown in Table 7.

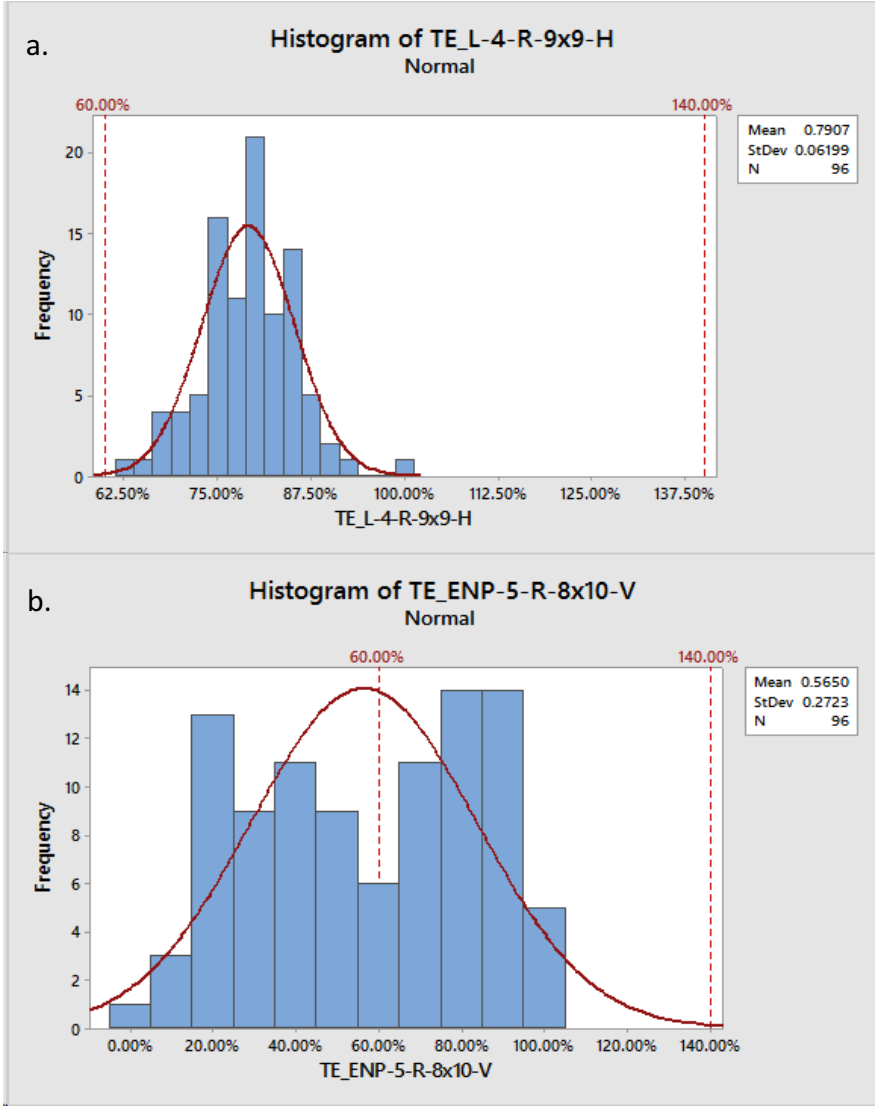

Figure 16. Histograms. This figure illustrates the distributions of the design with lower standard deviation (a) and the design with larger standard deviation (b).

Table 7

Selected designs.

		Selected Designs			Transfer Efficiency	
Manufacturing Type	Thick (mils)	Design	Size	Orientation	*Mean*	*St. Dev.*
Laser	4	Rounded	9x9	Horizontal	79.07%	6.20%
Electroforming with Nano-coating Polished	5	Rounded	8x10	Vertical	56.50%	27.23%

Identify the Operating Window

The two selected design were subjected to the operating window methodology. To start the experiment, the moderate noise level was applied. The nominal setting was the starting point for the sequential approach. At a first attempt, the squeegee speed was applied at 3 in. per second as the noise factor for the lower boundary. However, it was noticed that at this level, the noise was too detrimental to the system performance and poor results were found, even with a high squeegee pressure level. A new level of 2 in. per second for the squeegee speed was then adopted.

Starting with the design that presented the highest variation, the pressure levels were changed gradually and the results are shown in Table 8. The minimum volume calculated from the Schake and Whitmore (2016) equations for the 10x8 apertures is 1.63 nl. As the aperture volume for this design is 5.39 nl, the minimum transfer efficiency is found at 30%. This transfer efficiency level is used as a proxy to the real failure mode.

Table 8

High TE variation design results.

Threshold	Run	Speed	Cleaning	Pressure	TE
Lower	1	2.0	Yes	24.0	33%
Lower	2	2.0	Yes	24.0	46%
Lower	3	2.0	Yes	23.0	23%
Lower	4	2.0	Yes	22.0	26%
Lower	5	2.0	Yes	20.0	21%
Lower	6	2.0	Yes	15.0	19%
Lower	7	2.0	Yes	22.0	32%
Lower	8	2.0	Yes	21.0	27%
Lower	9	2.0	Yes	21.5	28%
Upper	1	0.5	No	24.0	43%
Upper	2	0.5	No	24.0	39%
Upper	3	0.5	No	25.0	56%
Upper	4	0.5	No	30.0	57%
Upper	5	0.5	No	32.0	58%
Upper	6	0.5	No	35.0	28%
Upper	7	0.5	No	35.0	50%
Upper	8	0.5	No	40.0	35%

From Table 8, it can be seen that when the pressure is reduced below 22 lbs., the distribution means drops below the 30% transfer efficiency, indicating that the failure limit was

reached for the lower threshold. For the upper limit, the same is not valid. The maximum transfer efficiency found was 58% for 32 lbs. After this maximum peak, it is possible to see a decrease in the transfer efficiency. With 58% of transfer efficiency being the maximum reached, it was not possible to find an upper threshold for the operating window.

The results from the experiment for the design that presented the lowest transfer efficiency variance are presented in Table 9. Using Schake and Whitmore (2016) equations for the 9x9 apertures, the minimum volume is 1.43 nl. As the aperture volume for this design is 4.79 nl., the minimum transfer efficiency is found at 30%. Coincidentally, the same value was found for both apertures, and the 30% transfer efficiency level was also used for the design with the narrow distribution.

Table 9

Low TE variation design results.

Threshold	Run	Speed	Cleaning	Pressure	TE
Lower	1	2.0	Yes	24.0	68%
Lower	2	2.0	Yes	22.0	51%
Lower	3	2.0	Yes	15.0	42%
Lower	4	2.0	Yes	10.0	46%
Lower	5	2.0	Yes	5.0	17%
Lower	6	2.0	Yes	7.0	44%
Lower	7	2.0	Yes	6.0	60%
Lower	8	2.0	Yes	6.0	46%
Upper	1	0.5	No	24.0	66%
Upper	2	0.5	No	26.0	62%
Upper	3	0.5	No	30.0	67%
Upper	4	0.5	No	35.0	64%
Upper	5	0.5	No	40.0	58%
Upper	6	0.5	No	37.0	49%
Upper	7	0.5	No	35.0	59%
Upper	8	0.5	No	30.0	64%
Upper	9	0.5	No	10.0	40%

The results for the lower limit shows that even a pressure as low as 6 lbs. gave results above the lower limit. Only at 5 lbs. the transfer efficiency dropped significantly. For the upper threshold, the maximum value was found at 30 lbs. The same pattern from the previous design was found for this design with the transfer efficiency dropping after a peak. Again, it was not possible to reach an upper threshold for the operating window. This pattern shows that other factor might be affecting the printing output and will be addressed in the discussion. Figure 17 shows the variance on the data from the Tables 8 and 9.

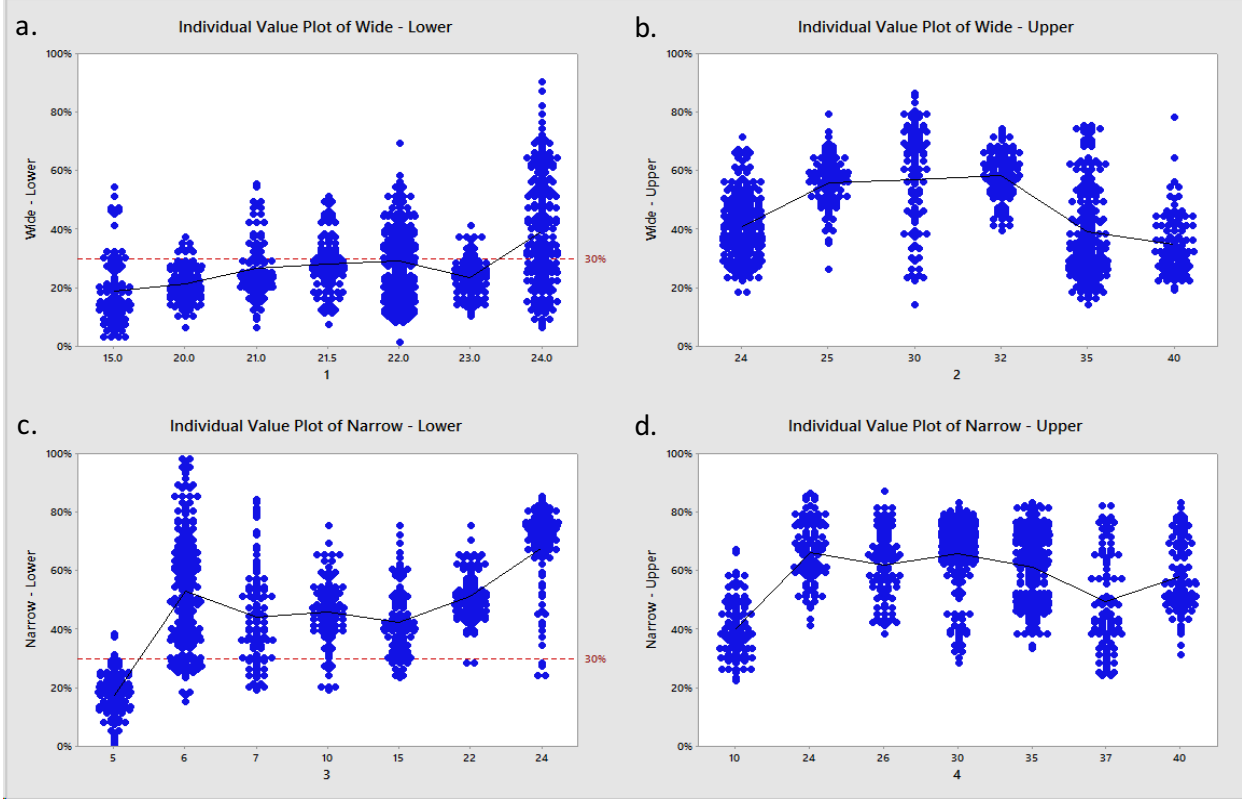

Figure 17. Operating window experiment result. This figure illustrates the distribution of the data when the level of the operating window factor varies for the lower (a) and upper (b) limits of the design with wide distribution and for the lower (c) and upper (d) limits of the design with narrow distribution.

On the chart for the lower threshold of the design with wide distribution (Figure 17a), it can be seen a high variability of the data, with an oscillatory mean. Only after 22 lbs. a pattern of a decreasing mean is present. It could be argued that before the 22 lbs. level, the mean varies around the operating window failure boundary and that the levels are as detrimental as the 22 lbs. level. It can also be seen a low variability as the mean approaches zero. The chart for the upper threshold (Figure 17b) presents an increase, a leveling and a decrease of the results. However, nothing could be concluded from the data scatter as it varies differently from level to level. From the charts for the lower threshold of the design with narrow distribution (Figure 17c), it can be seen a decrease and a leveling of the results. It can also be noted that the variation increases as we approximate the operating window boundaries. The last plot presents a small variation but it might be limited by its proximity to the zero. Finally, from the charts for the upper threshold (Figure 17d), it can be seen that the results increase from the first level to the others and then it is kept constant, with a decrease at the end. The excess of variability allows the argument that the results obtained on the 24 lbs. level is the same as the result obtained with 30 lbs., as the resulting mean distribution does not show a continuous pattern. The results are summarized on Figure 18. Both operating window are shown and a comparison is made. Note that both operating window have an undefined upper threshold.

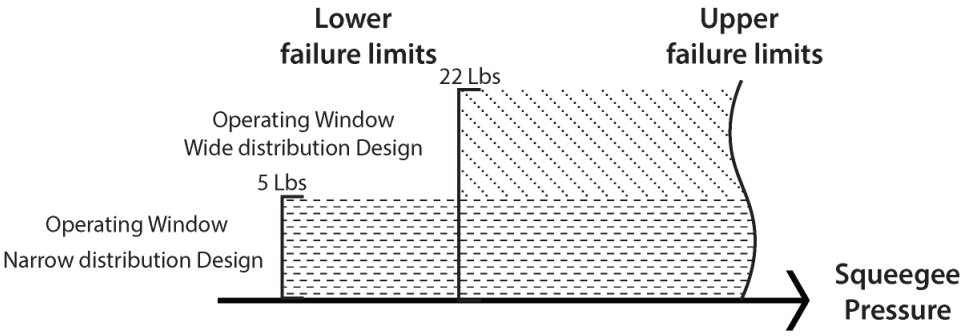

Figure 18. Operating window. This figure illustrates the operating window of the two designs studied.

Conclusions

The implementation of a method has to take into account the ease of comprehension and implementation by the users, it has to be consistency with the model being developed, and it has to consider the design characteristics of this model (Leitnaker and Mee, 2004). The proposed experimental approach has simple and intuitive steps. These characteristics enable an easy understanding by the readers and allow future replication. Different from the complex approaches proposed by previous research, the simplicity of the methodology applied enable the expansion of the operating window methodology. As proposed by Clausing (2004), one of the benefits of the operating window methodology should be its easy and intuitive application by engineering teams.

The available stencils and machinery enabled the successful replication of Mohanty et al. (2011) study. The same problem with the trapezoid shape apertures was found, indicating that this type of design is not adequate for the 01005 components. A complete statistical analysis was not performed but the results obtained in this study are consistent with Mohanty et al. (2011). It can be seen that higher TE is directly correlated with higher AR. In addition, the Electroformed with nano-coating polished stencils produced the highest mean for the four mils stencil designs and the laser with nano-coat presented the highest mean for the designs on the five mils stencil.

The first steps of the operating window methodology can be considered as the most important. Identifying the critical parameters, failure modes, and noise effects that are governed by the systems physics are key to the development of the operating window. Although experience can play a significant role in this process, the use of specific tools like FTA can help guide the identification process as is stated by Clausing & Fey (2004). Having a clear

understanding of the system physics without previous experience is a hard task. When not much experience has been developed in the process, the use of these auxiliary tools is essential to the system physics understanding. This was the case of this study. The experimenter did not have previous experience with the systems being analyzed. However, this is not true only for this project, as the development of the operating window is developed early in the system design phase, the knowledge from the entire system might not yet be developed. The importance of this process is confirmed on Blanchard & Fabrycky (2010) diagram.

From the experimental development it can be concluded that it is necessary to start the operating window methodology with a moderate level of noise, otherwise, the system that is not robust yet, will not be able to produce at acceptable levels. This confirms Clausing (2004) explanation that starting with a high noise level could hamper the system main functions if robustness is not developed into the system. The noise factors are applied to reduce the number of runs necessary. This was achieved by the experiment after the correction on the noise variable.

Because of the research objective, a one-dimensional operating window was analyzed. However, based on the critical parameters, failure modes, and noise effects identified, other configurations could be applied. From Figure 17, the change in pressure seems to have more impact on the lower limits than it does to the upper limit. A higher dimension operating window could have been an option to deal with this problem, as other factors might be more significant to the upper limit than the pressure. Squeegee speed, squeegee pressure, and the separation speed are identified as exerting greater influence on the printer performance. In this sense, a tridimensional operating window could be applied with these three factors. The development of this operating window would give a better understanding of the relationship between these

variables. In addition, would enrich the development process in terms of engineering. Future work could apply a higher degree operation window in terms of dimensions comparing the results with this research to understand what are the main factors on the decision of the dimension to be used, how this change the methodology process and how these changes impact the operating window outcome.

In addition, the use of a single replication of each run reduces the experimental time, but it also reduces the confidence of the results. As the objective of the study was not to find the exact value for the operating window thresholds, only one replication was used. In addition, as it was expected, the large difference from the lower boundaries of the two distribution can be sustained even without replications. However, to be able to determine small differences and for future work, it is recommended the development of replications for each run. The replications will enable a higher confidence on the mean results.

With the experiment developed it was possible to define the operating window for both designs. However, some caveats have to be considered. The results show a defined lower boundary for both distributions. For the design with larger variation, the lower threshold is defined at 22 lbs. For the design with smaller variation, the boundary is set at 5 lbs. The upper thresholds for both designs were not defined. For this research, a one-sided operating window was defined for both designs (Figure 18). However, the experiment shows that a possible failure that has not been identified might be affecting the upper boundaries. The results obtained show a significant difference between the boundaries values. More effort would be needed if these values were close to each other.

Two hypothesis were generated for the pattern found on the upper threshold. First, as the squeegee pressure increases beyond a certain value, the stencil starts bending and the part that

already received solder paste lift disconnecting from the PCB. This would generate a quick and not uniform release from the aperture, without the smoothness provided by the normal condition. The second hypothesis is that the squeegee itself bends on a high pressure. This would reduce the angle between the squeegee and the stencil, reducing the solder paste roll during the print. There was an attempt to test both hypothesis, but the right tools were not available. Future work could test both hypotheses by implementing a visual apparatus to record and measure the squeegee angle and stencil deformity during the print. Future work could also apply more specific reliability tools to identify if other factors affect the ability to find the upper operating window boundaries for this specific experiment.

Even with the limitations discussed above, it was still possible to confirm that a design with narrow distribution has an operating window larger than a design with a wide distribution. However, the proposed hypothesis confirmation does not prove that all designs with smaller standard deviation have a larger operating window when compared with the design with larger standard deviation. This work is just a first step showing the possibility of this relationship and future work is necessary to extend this hypothesis. With the development of a unique experiment, this research hopes to complete its objective of expanding the operating window methodology discussion.

References

Amalu, E. H., Lau, W. K., Ekere, N. N., Bhatti, R. S., Mallik, S., Otiaba, K. C., & Takyi, G. (2011). A study of SnAgCu solder paste transfer efficiency and effects of optimal reflow profile on solder deposits. *Microelectronic Engineering, 88*(7), 1610-1617. doi:10.1016/j.mee.2011.02.104

Armillotta, A., & Semeraro, Q. (2013). Critical operating conditions for assemblies with parameter-dependent dimensions. *Proceedings of the Institution of Mechanical Engineers, Part B: Journal of Engineering Manufacture, 227*(5), 735–744. http://doi.org/10.1177/0954405412472640

Bergman, B., de Mare, J., & Svensson, T. (2009). *Robust design methodology for reliability: exploring the effects of variation and uncertainty*. Hoboken, NJ: John Wiley & Sons.

Bernardo, F. P., & Saraiva, P. M. (1998). Robust optimization framework for process parameter and tolerance design. *AIChE Journal, 44*(9), 2007–2017. Retrieved from http://www.scopus.com/scopus/inward/record.url?eid=2-s2.0-0032172413&partnerID=40&rel=R8.2.0

Blanchard, B. S., & Fabrycky, W. (2010). *Systems engineering and analysis* (5th ed.). Englewood Cliffs, NJ: Prentice Hall.

Box, G. E. P., Hunter, J. S., & Hunter, W. G. (2005). *Statistics for experimenters: Design, innovation, and discovery* (2nd ed.). Hoboken, NJ: Wiley-Interscience.

Clausing, D. P. (2004). Operating window: An engineering measure for robustness. *Technometrics, 46*(1), 25–29. http://doi.org/10.1198/004017004000000077

Clausing, D. P., & Fey, V. (2004). *Effective innovation*. New York, NY: ASME Press.

Creveling, C. (1997). *Tolerance design: A handbook for developing optimal specifications*.

Reading, MA: Addison-Wesley.

Crosby, P. B. (1979). *Quality is free: The art of making quality certain*. New York, NY: McGraw-Hill.

Czitrom, V. (1999). One-Factor-at-a-Time Versus Designed Experiments. *American Statistical Association*, *53*(2), 6. http://doi.org/10.2307/2685731

Daniel, C. (1973). One-at-a-Time Plans. *Journal of the American Statistical Association*, *68*(342), 353–360. Retrieved from http://www.jstor.org/stable/2284076

Feigenbaum, A. V. (1991). *Total quality control* (3rd ed.). New York, NY: McGraw-Hill.

Frey, D. D., & Jugulum, R. (2006). The Mechanisms by Which Adaptive One-factor-at-a-time Experimentation Leads to Improvement. *Journal of Mechanical Design*, *128*(5), 1050. http://doi.org/10.1115/1.2216733

Fowlkes, W. Y., & Creveling, C. M. (1995). *Engineering methods for robust product design: Using taguchi methods in technology and product development.* Reading, MA: Addison-Wesley.

Friedman, M., & Savage, L. J. (1947). Planning experiments seeking maxima. In *Selected Techniques of statistical analysis: for scientific and industrial research and production and management engineering* (1st ed., pp. 363–372). New York, NY: McGraw-Hill.

Gryna, F. M., Chua, R. C. H., De Feo, J. A., & Juran, J. M. (2007). *Juran's quality planning and analysis: For enterprise quality* (5th ed.). New York, NY: McGraw-Hill.

Herron, J. C., Hodgson, P. D., & Cardew-Hall, C.-H. (1998). Defining the operating window for an automotive sheet pressing operation. *Journal of Materials Processing Technology, 80-81*, 68–75. http://doi.org/10.1016/S0924-0136(98)00100-9

Hoyle, D. (2005). *Automotive quality systems handbook: ISO/TS 1649:2002 edition* (2nd ed.).

Burlington, MA; Elsevier Butterworth-Heinemann.

Hur, J., Jeon, M.-Y., Kim, H.-M., Yun, S.-K., & Hong, J. (2014). Three Dimentional Shape Measurement Apparatus. *U.S. Patent No. 8,754,936*. Washington, DC: U.S. Patent and Trademark Office.

Joseph, V. R., & Wu, C. F. J. (2002). Operating window experiments: A novel approach to quality improvement. *Journal of Quality Technology, 34*(4), 345–354. Retrieved from http://search.proquest.com.ezproxy.rit.edu/docview/214489954?accountid=108

Joseph, V. R., & Wu, C. F. J. (2004). Failure amplification method: An information maximization approach to categorical response optimization. *Technometrics, 46*(1), 1–12. http://doi.org/10.1198/004017004000000013

Juran, J. M., & Godfrey, A. B. (1998). *Juran's quality control handbook* (5th ed.). New York, NY: McGraw-Hill.

Leitnaker, M. G., & Mee, R. W. (2004). Discussion. *Technometrics, 46*(1), 12–14. http://doi.org/10.1198/004017004000000022

La Vallee, L. (1992), Application of Taguchi Robust Design Method to the Design of Friction Retard Feeder. In *Selected Case Studies in the Use of Tolerance and Deviation Information During Design of Representative Industrial Products* (1st ed., pp. 65–95). New York, NY: ASME Press.

Logothetis, N., & Wynn, H. P. (1994). *Quality through design: experimental design, off-line quality control, and Taguchi's contributions* (7th ed.). New York, NY: Oxford University Press.

Mangin, C. (1991, February). Where quality is lost on SMT boards. *Circuits Assembly*, 63–64.

McClusky, R. (2000). The rise, fall and revival of six sigma quality. *Quality Focus*, 4(2), 6-17.

Retrieved from http://search.proquest.com.ezproxy.rit.edu/docview/208744470?accountid=108

McDaniel, W. R., & Ankenman, B. E. (2000). Comparing experimental design strategies for quality improvement with minimal changes to factor levels. *Quality and Reliability Engineering International*, *16*(5), 355–362. http://doi.org/10.1002/1099-1638(200009/10)16:5<355::AID-QRE344>3.0.CO;2-I

Meeker, W. Q., & Escobar, L. A. (2004a). Discussion. *Technometrics, 46*(1), 15–16. http://doi.org/10.1198/004017004000000031

Meeker, W. Q., & Escobar, L. A. (2004b). Reliability: The other dimension of quality. *Quality Technology & Qualitative Management, 1*(1), 1–25. Retrieved from http://web.it.nctu.edu.tw/~qtqm/qtqmpapers/2004V1N1/2004V1_F1.pdf

Mohanty, R., Ramkumar, M., Anglin, C., Oda, T., & Mark, B. (2011). Effect of Nano-Coated Stencil on 01005 Printing. In *IPC APEX EXPO Technical Conference* (pp. 1727–1736). Las Vegas, NV.

Montgomery, D. C. (2013). *Design and analysis of experiments* (8th ed.). New York, NY: John Wiley & Sons.

Mori, T. (1995). *Taguchi Techniques for Image and Pattern Development Technology.* Englewood Cliffs, NJ: Prentice Hall.

Mori, T., & Tsai, S.-C. (2011). *Taguchi methods: Benefits, impacts, mathematics, statistics, and applications.* New York, NY: ASME Press. http://doi.org/10.1115/1.859698

Nair, V. N., Abraham, B., MacKay, J., Nelder, J. a, Box, G., Phadke, M. S., … Wu, C. F. J. (1992). Taguchi's parameter design: A panel discussion. *Technometrics, 34*(2), 127. http://doi.org/10.2307/1269231

Omori, M. K., & Miller, F. G. (1992). Solder paste stencil printer. *U.S. Patent No. 5,107,759*. Washington, DC: U.S. Patent and Trademark Office.

Pan, J. (2006). Evaluating the gauge repeatability and reproducibility for different industries. *Quality & Quantity, 40*(4), 499-518. doi:10.1007/s11135-005-1100-y

Peace, G. S. (1993). *Taguchi Methods: A Hands-On Approach*, Reading, MA: Addition-Wesley.

Prasad, R. P. (1997). *Surface mount technology* (2nd ed.). Boston, MA: Springer US. http://doi.org/10.1007/978-1-4615-4084-7

Qu, X., & Jeff Wu, C. F. (2005). One-factor-at-a-time designs of resolution V. *Journal of Statistical Planning and Inference*, *131*(2), 407–416. http://doi.org/10.1016/j.jspi.2004.03.002

Roy, R. K. (2010). *A primer on the Taguchi method* (2nd ed.). Dearborn, MI: Society of Manufacturing Engineers.

Schake, J., & Whitmore, M. (2016). First Look at Printing Metric 0201' s. In *International Conference on Soldering and Reliability Conference*. Toronto, ON: SMTA.

Schenkelberg, F. (2013). Establishing product reliability goals. In *2013 Proceedings Annual Reliability and Maintainability Symposium (RAMS)* (pp. 1–6). Orlando, FL: IEEE. http://doi.org/10.1109/RAMS.2013.6517741

Sharma, N. K., & Cudney, E. a. (2009). Signal-to-Noise ratio for operating window using unified methodology. *Concurrent Engineering, 17*(3), 173–181. http://doi.org/10.1177/1063293X09343334

Shu, M.-H., Cheng, C.-H., & Chang, J.-R. (2006). Using intuitionistic fuzzy sets for fault-tree analysis on printed circuit board assembly. *Microelectronics Reliability*, *46*(12), 2139–2148. http://doi.org/10.1016/j.microrel.2006.01.007

Speedline Technologies. (2016). MPM momentum series. Retrieved June 28, 2016, from http://www.speedlinetech.com/

Taguchi, G. (1986). *Introduction to quality engineering: Designing quality into products and processes.* Tokyo, Japan: Asian Productivity Organization.

Taguchi, G. (1993). *Taguchi on robust technology development*. New York, NY: ASME Press. http://doi.org/10.1115/1.800288

von Hippel, E. (1998). Economics of product development by users: The impact of "sticky" local information. *Management Science*, 44(5), 629-644. doi:10.1287/mnsc.44.5.629

Wallace, K., & Clarkson, J. (1999). *An introduction to the design process*. Cambridge, UK. Retrieved from http://www-mdp.eng.cam.ac.uk/web/library/enginfo/design/design_process.pdf

Wu, C.-F., & Hamada, M. (2009). *Experiments: planning, analysis, and optimization* (2nd ed.). Hoboken, NJ: Wiley-Interscience.

Yang, G. (2007). *Life cycle reliability engineering*. Hoboken, NJ: John Wiley & Sons.

Appendix A

Fault Tree Analysis

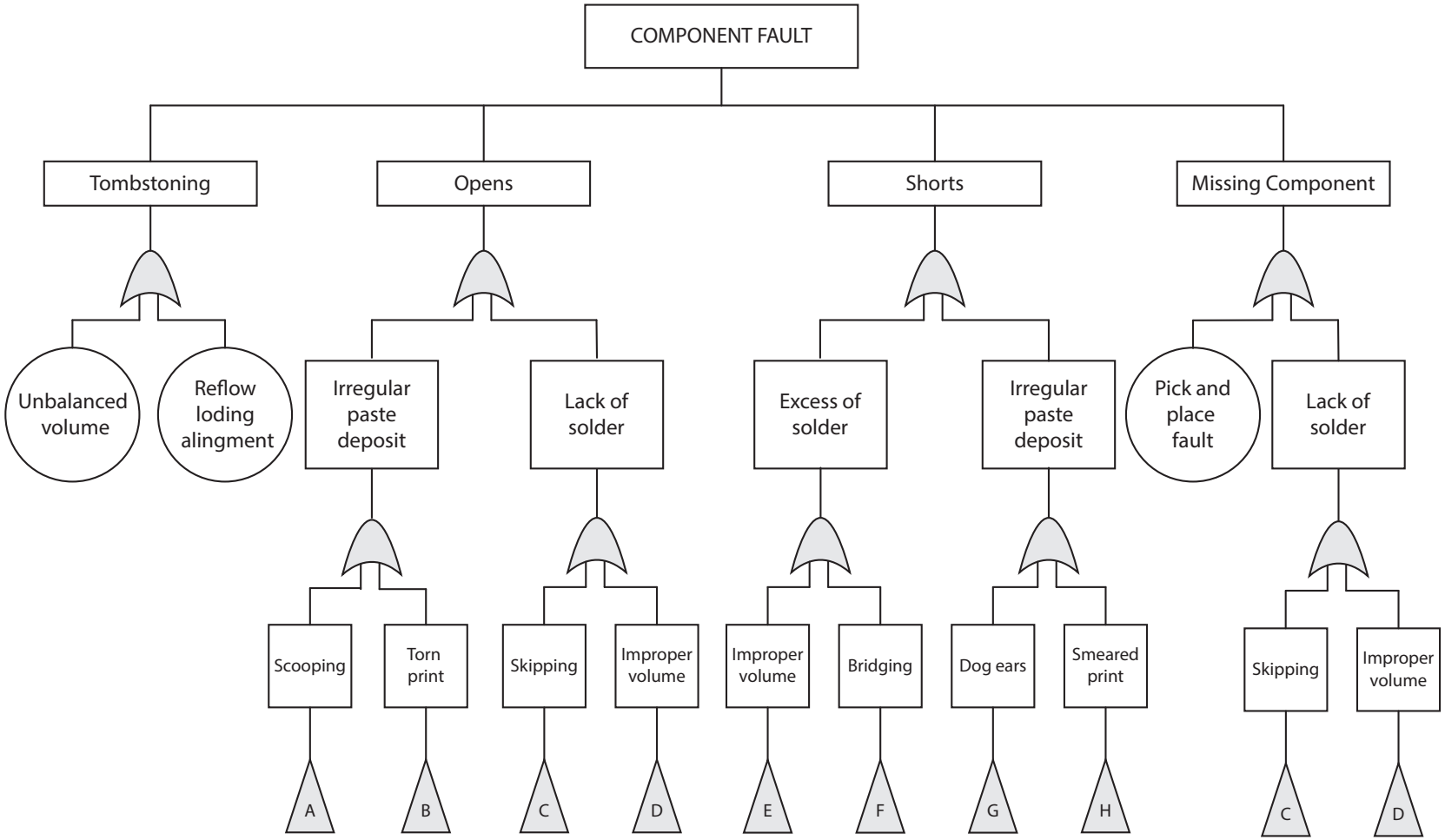

Figure A1. FTA. This figure illustrates the Fault Tree Analysis from PCB components

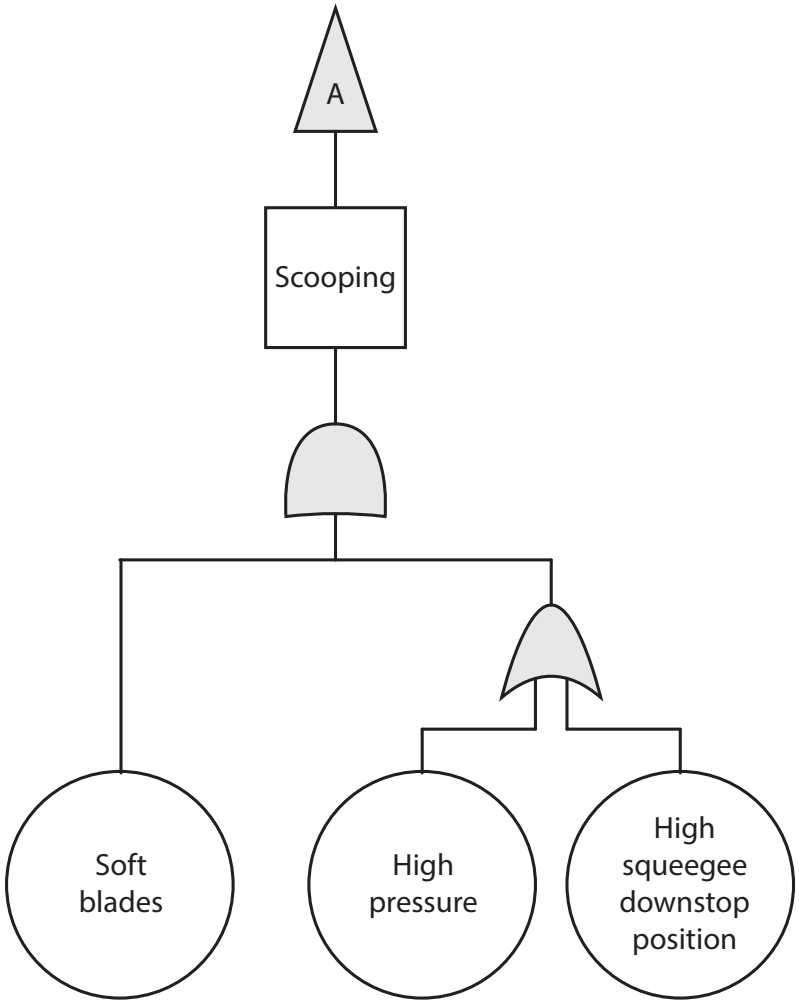

Figure A2. FTA path A. This figure illustrates the continuation of the FTA from PCB component

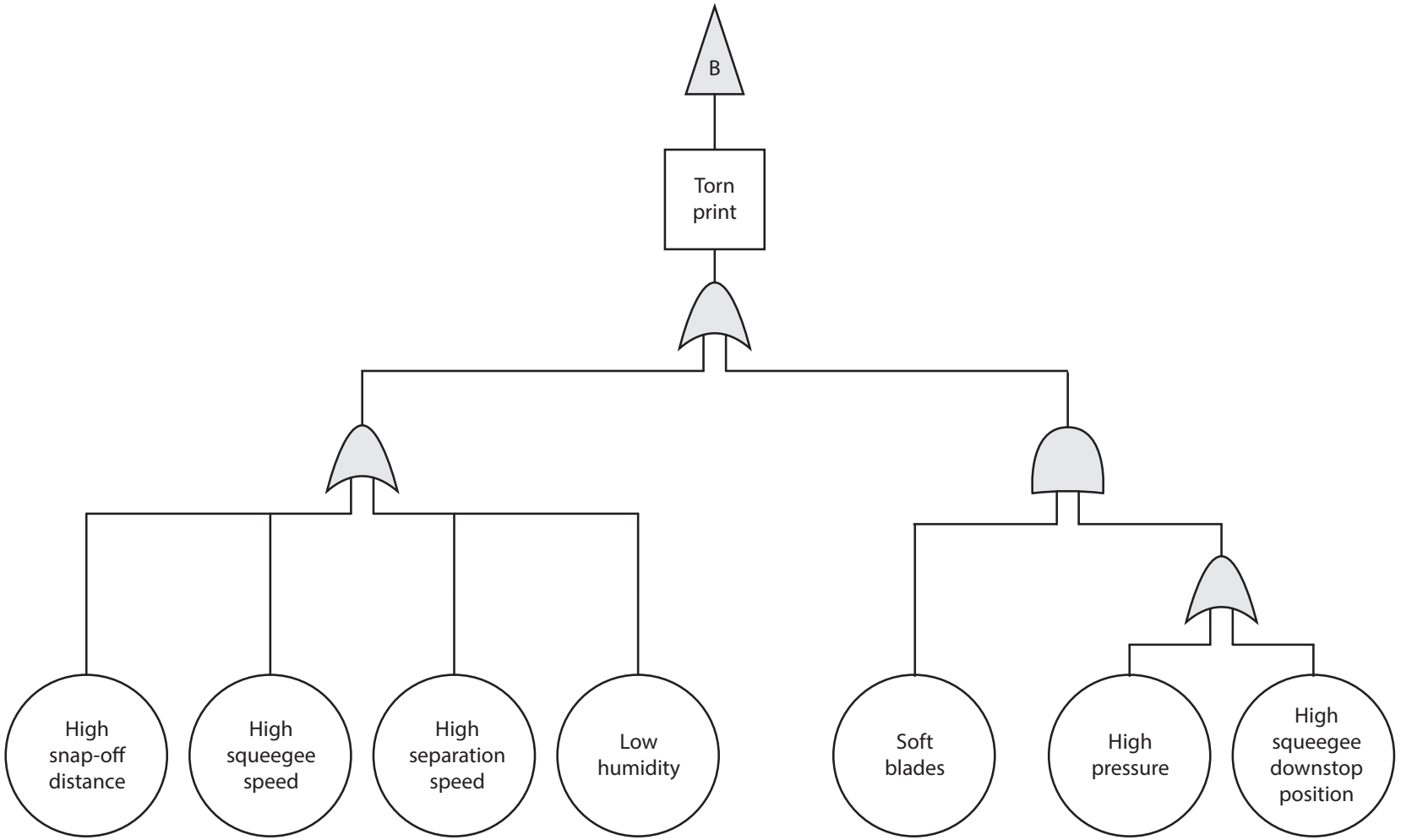

Figure A3. FTA path B. This figure illustrates the continuation of the FTA from PCB components.

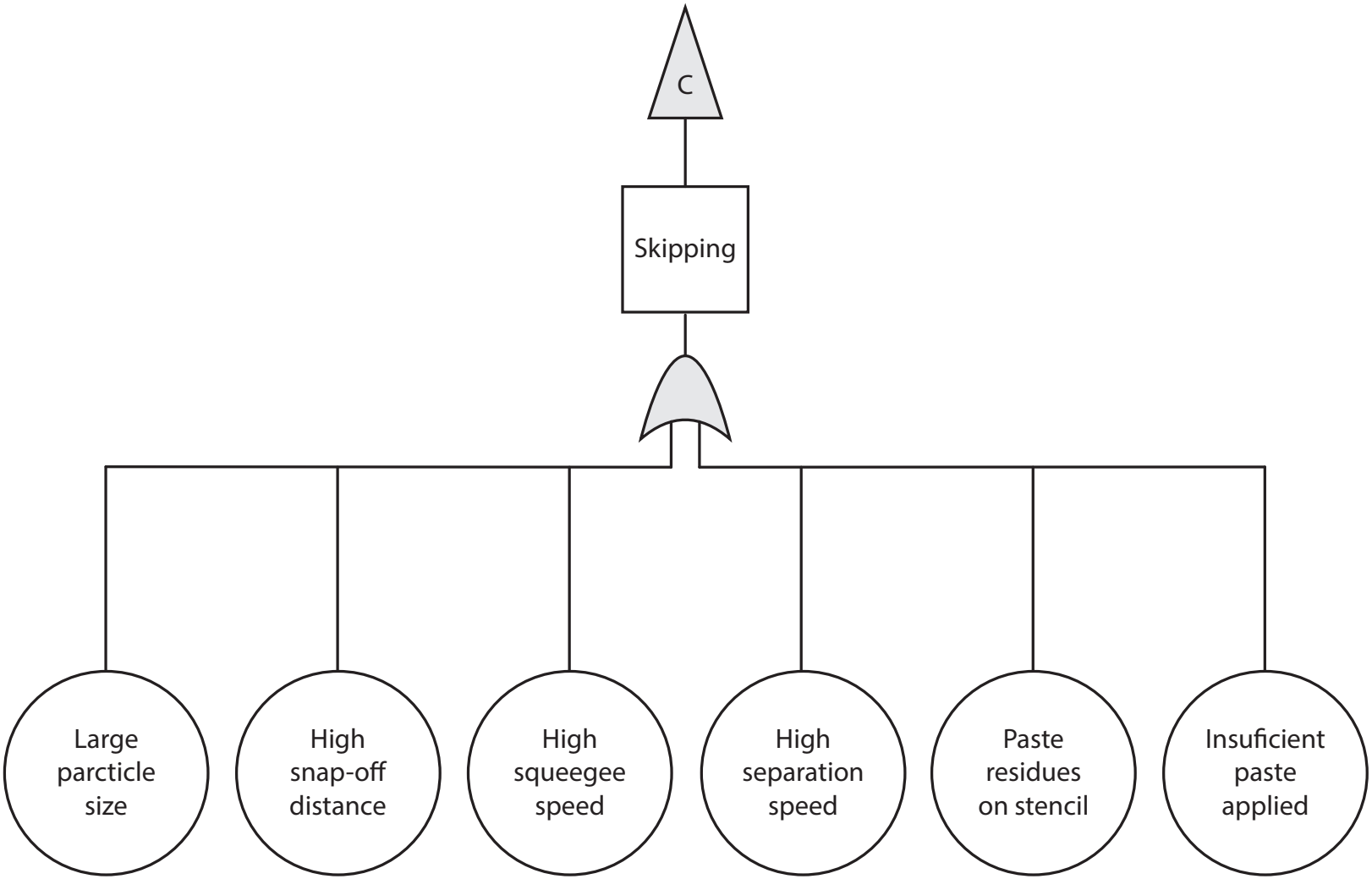

Figure A4. FTA path C. This figure illustrates the continuation of the FTA from PCB components.

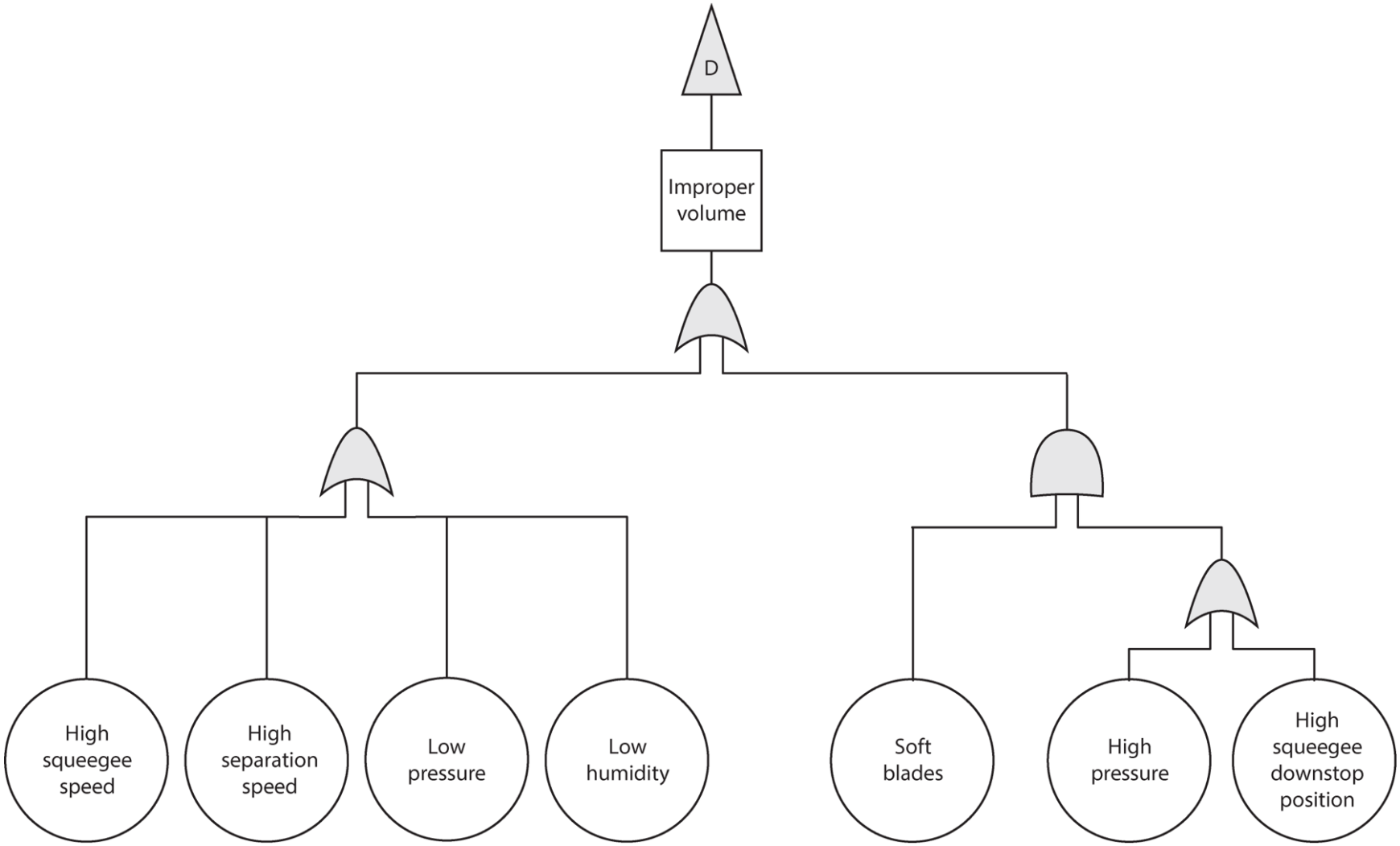

Figure A5. FTA path D. This figure illustrates the continuation of the FTA from PCB components.

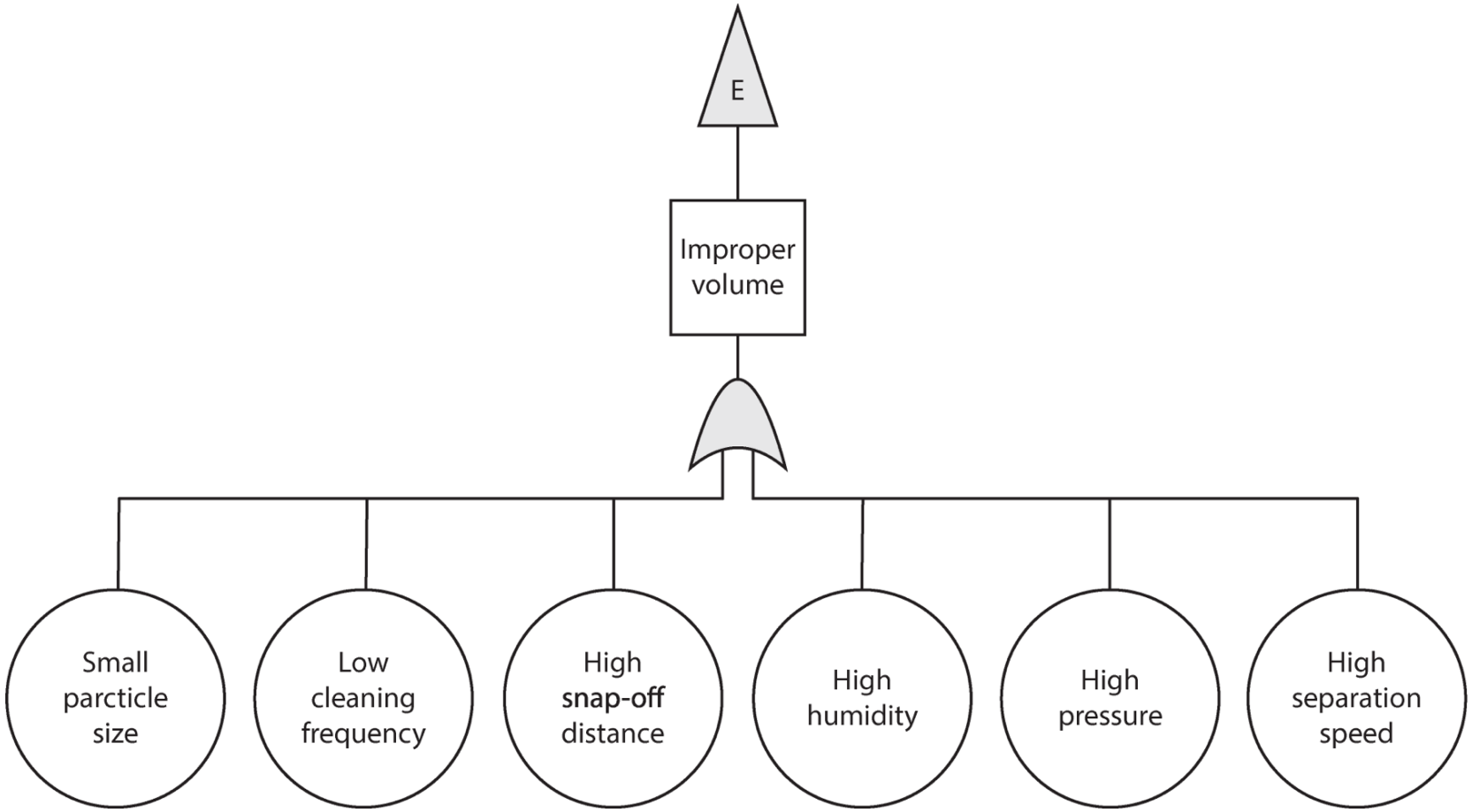

Figure A6. FTA path E. This figure illustrates the continuation of the FTA from PCB components.

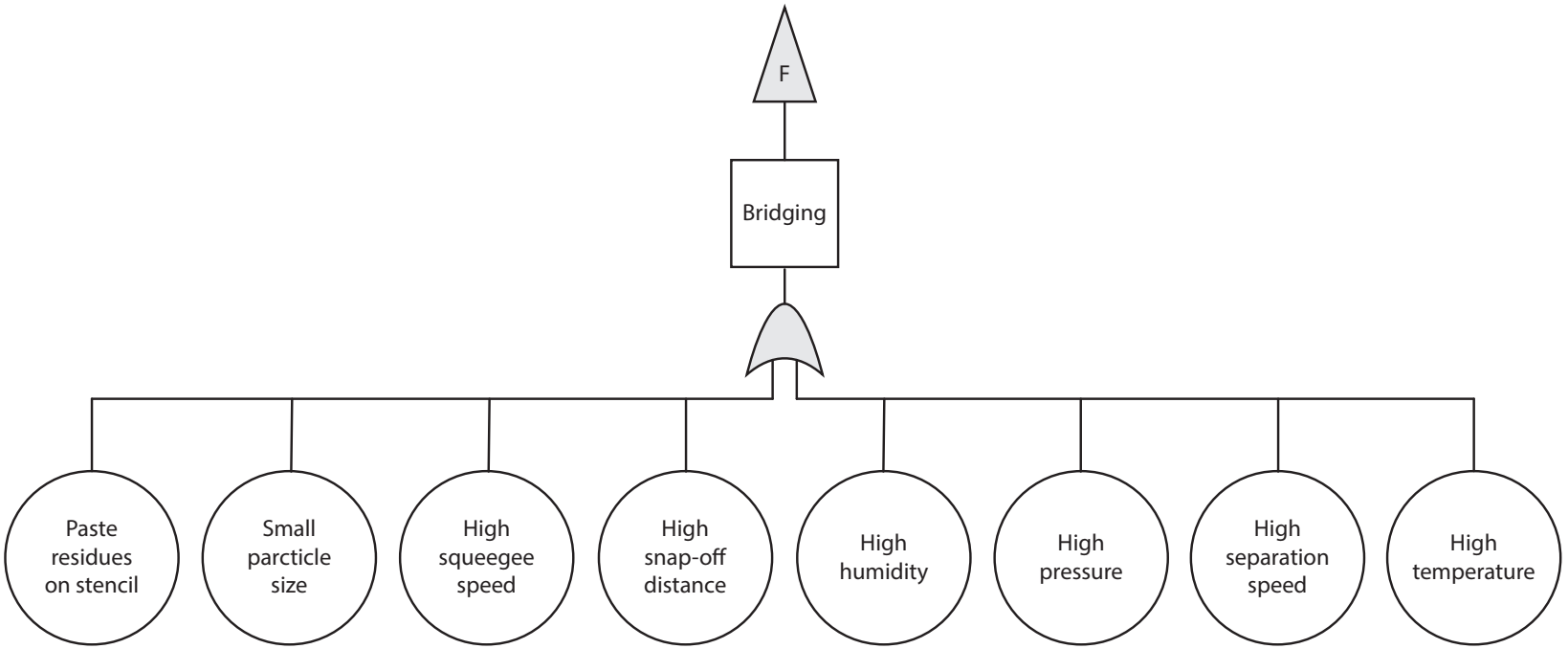

Figure A7. FTA path F. This figure illustrates the continuation of the FTA from PCB components.

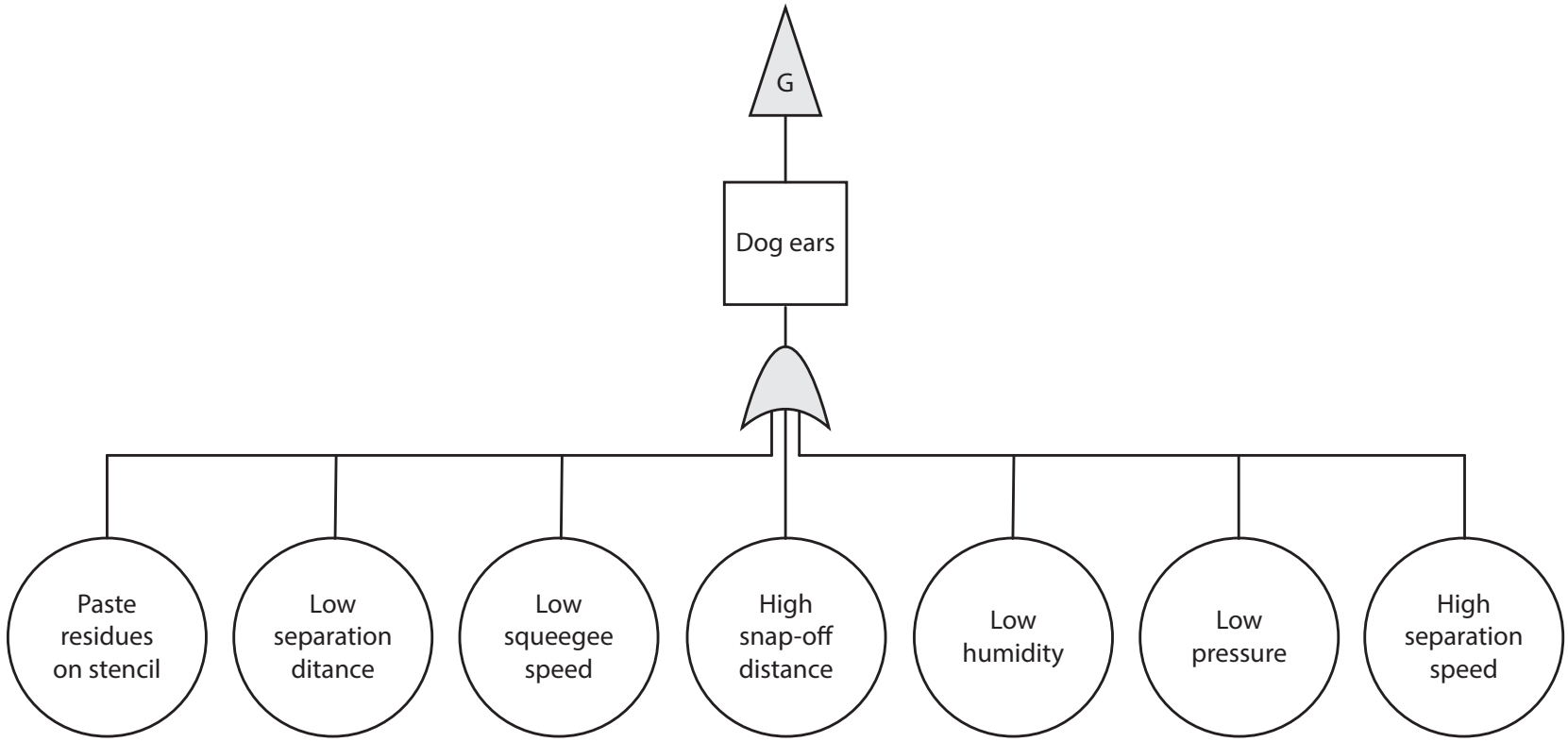

Figure A8. FTA path G. This figure illustrates the continuation of the FTA from PCB components.

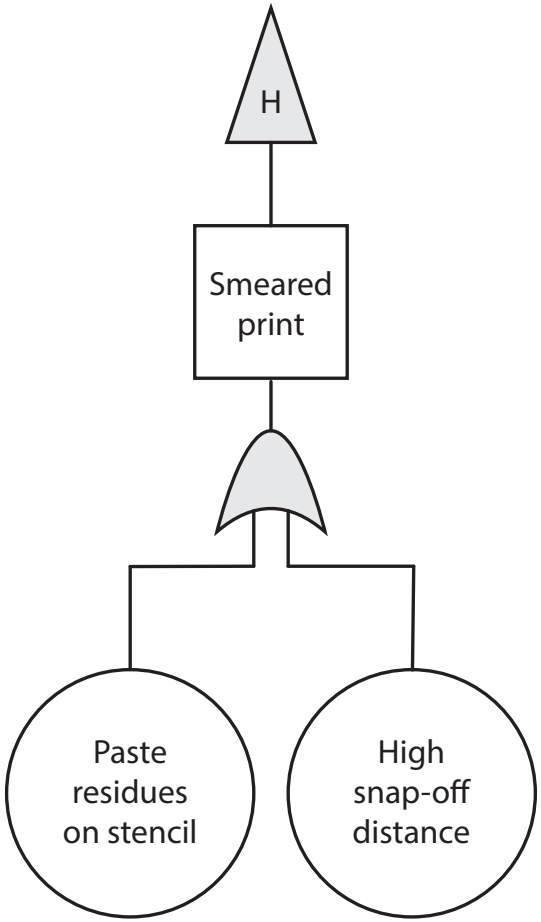

Figure A9. FTA path H. This figure illustrates the continuation of the FTA from PCB components.

Appendix B

Table B1

MPM Momentum Specifications. Retrieved June 28, 2016 from http://www.speedlinetech.com. Copyright 2016 by the Illinois Tool Works.

BOARD HANDLING		PERFORMANCE	
Maximum Board Size (X x Y)	609.6 mm x 508 mm (24” x 20”)	Total System Alignment Accuracy and Repeatability	±12.5 microns (±0.0005") at 6 sigma, Cpk ≥ 2.0*
Staging Mode - Momentum Elite	457 mm x 508 mm (18” x 20”)	Qualification is performed using production environment process variables; print speed, table lift and camera movement are included in the capability figure.	
A dedicated workholder is required for boards with an X size greater than 20”			
Minimum Board Size (X x Y)	50.8 mm x 50.8 mm (2” x 2”)	Wet Print Deposit Accuracy and Repeatability	±20 microns (±0.0008") at 6 sigma, Cpk ≥ 2.0*
Board Thickness	0.2mm (0.008”) to 5.0mm (0.20”), up to 6.0 mm (0.24”) without top clamp foils	Based upon actual wet printing with positional accuracy and repeatability verified by a 3rd party measurement system.	
		Cycle Time	
Maximum Board Weight	4.5 kg (10 lbs)	Momentum HiE	7.5 seconds standard
Board Edge Clearance	3.0 mm (0.118")	Momentum Elite	6.0 seconds standard
Underside Clearance	12.7 mm (0.5") standard Configurable for 25.4 mm (1.0”)	FACILITIES	
		Power Requirements	200 to 240 VAC (±10%) single phase @ 50/60Hz, 15A
Board Hold-Down	Fixed top clamps, centernest vacuum, EdgeLoc (Optional on HiE)	Air Supply Requirements	100 psi at 4 cfm (standard run mode) to 18 cfm (vacuum wipe) (6.89 bar @ 1.9 L/s to 8.5 L/s), 12.7 mm (0.5”) diameter line

		Height (excluding light tower)	1638.4 mm (64.5") at 940 mm (37.0”) transport height
Board Support Methods	Magnetic pins Optional: Vacuum side dams, vacuum pins, support blocks, dedicated fixtures, patented auto tooling, Quik-Tool	Machine Depth	1593.1 mm (62.72")
		Machine Width	
PRINT PARAMETERS		Momentum HiE	1202.7 mm (47.35”)
Maximum Print Area (X x Y)	609.6 mm x 508 mm (24” x 20")	Momentum Elite	1675.5 mm (65.96”)
Print Gap (Snap-off)	0 mm to 6.35 mm (0" to 0.25")	Minimum Front Clearance	508 mm (20.0”)
Print Speed	Up to 305 mm/sec (12.0”/sec)	Minimum Rear Clearance	508 mm (20.0”)
Print Force	0 to 20 kg (0 lb to 44 lbs)	Machine Weight	
Stencil Frame Size	737 mm x 737 mm (29" x 29") Adapters available for smaller sizes	Momentum HiE	862 kg (1900 lbs)
VISION		Momentum Elite	899 kg (1982 lbs)
Vision Field-of-View (FOV)	10.6 mm x 8.0 mm (0.417” x 0.315”)	Crated Weight	
Fiducial Types	Standard shape fiducials (see SMEMA standards), pad/aperture	Momentum HiE	1155.5 kg (2547 lbs)
Camera System	Single digital camera - MPM patented look up/ down vision	Momentum Elite	1192.5 kg (2629 lbs)

* The higher the Cpk, the lower the variability with respect to the process specification limits. In a process qualified as a 6 sigma process (i.e., one that allows plus or minus 6 standard deviations within the specification limits), the Cpk is greater than or equal to 2.0.

Specification is subject to change without notice. Please consult factory for specifics.

Speedline maintains an ongoing program of product improvement that may affect design and/or price. We reserve the right to make these changes without prior notice or liability.

Appendix C

Table C1

OGP Flashscope Quest 650 Specifications. Retrieved June 28, 2016 from http://kohyoung.com/en/ky-3020t/.

	Standard	Optional
XYZ travel	610 x 660 x 400 mm	
XYZ scale resolution	0.1 μm	0.05 μm; 0.04 μm
Drive system	XY liquid cooled linear motor drives; Z and zoom, DC servo	
Worktable	Hardcoat anodized, with fixture holes, removable stage glass, 100 kg recommended max payload	
Optics	Patented† 10:1 AccuCentric® TeleStar® auto-calibrating, telecentric zoom, motorized; mag range 0.8x-8x, with up to 10 calibrated positions; 1.0x replacement lens	Replacement lenses, optical: 0.45x/200 mm WD, 0.5x/130 mm WD, 2.0x/32 mm WD, 4.0x/20 mm WD Replacement lenses, optical/laser: 0.45x/200 mm WD, 0.5x/130 mm WD, 2.0x, 4.0x Optical accessories: LED grid projector, laser pointer (not available w/TTL laser)
FOV size (std opitical configuration)	Measured diagonally, 8.9 mm (low mag) to 0.9 mm (high mag)	
Illumination	Patented†† high performance monochromatic substage backlight, LED coaxial TTL surface, 8 sector/6 ring SmartRing™ LED	
Camera	High resolution, black & white digital metrology camera	High resolution color metrology camera
Image processing	256 level grayscale processing with 10:1 subpixel resolution	
Sensor options (contact OGP for possible combinations of sensors)		Touch probe and change rack, SP25 scanning probe, patented††† on-axis TeleStar Plus interferometric TTL laser, off-axis DRS™ laser, Feather Probe™, Rainbow Probe™ scanning white light sensor, PH10 motorized probe head
Controller	Windows® based, with up-to-date processor and networking/communication ports	
Controller accessory package	24” flat panel LCD monitor, keyboard, 3-button mouse	24” flat panel LCD monitor for dual monitor display

Software	QVI Portal, including: • Portal Navigator • Independent Calibration Engine (ICE) • Multimedia Content Viewer • SmartLink™	Metrology software: ZONE3® or ZONE3 Pro, MeasureMind® 3D MultiSensor Productivity software: MeasureFit® Plus, SmartFit® 3D, SmartProfile® Offline software: ZONE3, MeasureMind 3D MultiSensor
Power requirements	230 vac, 50/60 Hz, 1 phase, 1550 W; Air - clean, dry air at 80 PSI min, 7 SCFM flowrate	
Rated environment	Temperature 18-22° C, stable to ±1° C; 30-80% humidity; vibration <0.001g below 15 Hz	
Operating environment, safe operation	15-30° C	
XYZ volumetric accuracy[1]	$E_3 = (1.8 + 5L/1000)$ µm[2,4,5]	$E_3 = (1.2 + 6L/1000)$ µm[2,4,5]
XY area accuracy[1]	$E_2 = (1.5 + 4L/1000)$ µm[2,3,4]	$E_2 = (1.0 + 5L/1000)$ µm[2,3,4] (requires optional 0.05 µm or 0.04 µm scale resolution)
Z linear accuracy[1]	$E_1 = (2.5 + 5L/1000)$ µm[4]	$E_1 = (1.5 + 5L/1000)$ µm[4] (with optional 2.0x replacement lens and grid projector; on-axis TeleStar Plus TTL laser; off-axis DRS-300 or -500 laser, or TP20 or TP200 touch probe)

†Patent Number 6,292,306 ††Patent Number 6,488,398 †††Patent Number 7,791,731

[1]Where L = measuring length in mm. Applies to thermally stable system in rated environment. Maximum rate of temperature change: 1° C/hour. Maximum vertical temperature gradient: 1° C/meter. All optical accuracy specifications at maximum zoom lens setting. Volumetric accuracy performance requires use of QVI 3D metrology software, such as MeasureMind 3D or ZONE3.

[2]With evenly distributed load up to 10 kg. Depending on load distribution, accuracy at maximum rated load may be less than standard accuracy.

[3]Measured in the standard measuring plane. The standard measuring plane is defined as a plane that is within 25 mm of the worktable surface.

[4]E_1 Z axis linear, E_2 XY area, and E_3 XYZ volumetric accuracy standards are described in QVI Publication Number 790762.

[5]On-site verification optional.

Appendix D

Table D1

Koh Young KY-3020T Specifications. Retrieved June 28, 2016 from https://www.ogpnet.com/north-america/systems/video-multisensor/smartscope-quest/smartscope-quest-650/index. Copyright 2015 by Quality Vision International, Inc.

Inspection Range			
Metrology Capability		Volume, Area, Height, Offset, Bridging and Shape Deformity	
Types of Defects		Insufficient/Excessive/Missing Paste, Bridging, Shape Deformity and Paste Offset	
Measurement Principle		3D Shadow Free Moiré	
Camera Technology			
Camera		1MPix	
XY Pixel Resolution		20 μm	0.79 mils
Z Resolution		0.37 μm	0.015 mils
Inspection Performance			
Inspection Speed at 20 μm		3 cm2/sec	0.47 sq. inch/sec
Volume Repeatability (on a KY Calibration Target)		< 1% at 3 σ	
Volume Repeatability (on a PCB)		< 3% at 3 σ	
Height Accuracy (on a KY Calibration Target)		2 μm	
Gage R&R (± 50 tolerance)		<< 10 % at 6 σ	
Max. PCB Warp Compensation		± 3.5 mm	0.14 inch
Max. Paste Height		400 μm	15.75 mils
Min. Paste Deposit Size at 20 μm	Rectangle	150 μm	5.91 mils
	Circle	200 μm	7.87 mils
Min. Distance between Paste Deposit		100 μm (at 150 μm paste height)	3.94 mils (at 5.91 mils paste height)
PCB Handling			
Conveyor Width Adjustment		Manual	
Conveyor Fix Type		Front/Rear Fixed (Factory Setting)	
Conveyor Height		N/A	
System & Installation requirements			
Supply	Electrical	200~240VAC, 50/60 Hz Single phase	
	Air	N/A	
Operating System		Windows XP Professional	

S/W	
Statistical Analysis Tool	SPC Plus
Inspection Program Generation	Import GERBER Data (274X, 274D)
Options	
	• ODB++ File Conversion • Handheld Barcode Reader (1D/2D) • Certified Calibration Target • UPS

Appendix E

Table E1

Experimental Results.

Designs					Transfer Efficiency	
Manufacturing Type	Stencil Thickness	Aperture Design	Aperture Size	Aperture Direction	Mean	Standard Deviation
EN	4	R	8x10	H	80.70%	7.82%
EN	4	R	8x10	V	80.09%	8.77%
EN	4	R	9x9	H	81.01%	7.33%
EN	4	R	9x9	V	81.10%	8.05%
EN	4	S	8x10	H	76.54%	6.42%
EN	4	S	8x10	V	76.28%	7.53%
EN	4	S	9x9	H	73.63%	7.11%
EN	4	S	9x9	V	76.97%	7.63%
EN	4	T	8x10	H	37.78%	10.48%
EN	4	T	8x10	V	38.85%	10.51%
EN	4	T	9x9	H	39.25%	9.95%
EN	4	T	9x9	V	39.10%	10.70%
EN	5	R	8x10	H	61.07%	19.30%
EN	5	R	8x10	V	60.65%	13.76%
EN	5	R	9x9	H	59.12%	18.37%
EN	5	R	9x9	V	61.24%	17.40%
EN	5	S	8x10	H	52.96%	16.31%

EN	5	S	8x10	V	55.45%	13.61%
EN	5	S	9x9	H	50.41%	16.54%
EN	5	S	9x9	V	53.36%	15.43%
EN	5	T	8x10	H	16.82%	8.02%
EN	5	T	8x10	V	16.58%	7.20%
EN	5	T	9x9	H	16.33%	7.26%
EN	5	T	9x9	V	15.09%	6.19%
ENP	4	R	8x10	H	96.48%	11.56%
ENP	4	R	8x10	V	96.98%	14.16%
ENP	4	R	9x9	H	94.39%	10.98%
ENP	4	R	9x9	V	96.24%	13.05%
ENP	4	S	8x10	H	90.10%	10.84%
ENP	4	S	8x10	V	91.27%	13.22%
ENP	4	S	9x9	H	85.68%	13.39%
ENP	4	S	9x9	V	88.11%	12.11%
ENP	4	T	8x10	H	29.12%	14.50%
ENP	4	T	8x10	V	33.03%	14.11%
ENP	4	T	9x9	H	26.45%	12.59%
ENP	4	T	9x9	V	34.89%	15.61%
ENP	5	R	8x10	H	57.58%	24.49%
ENP	5	R	8x10	V	56.50%	27.23%
ENP	5	R	9x9	H	56.59%	24.62%
ENP	5	R	9x9	V	55.92%	26.86%

ENP	5	S	8x10	H	51.64%	25.67%
ENP	5	S	8x10	V	46.48%	23.09%
ENP	5	S	9x9	H	45.19%	24.71%
ENP	5	S	9x9	V	49.47%	26.27%
ENP	5	T	8x10	H	10.32%	7.59%
ENP	5	T	8x10	V	6.53%	6.52%
ENP	5	T	9x9	H	9.76%	6.34%
ENP	5	T	9x9	V	11.32%	6.87%
L	4	R	8x10	H	83.06%	6.42%
L	4	R	8x10	V	80.48%	8.83%
L	4	R	9x9	H	79.07%	6.21%
L	4	R	9x9	V	78.89%	8.41%
L	4	S	8x10	H	78.88%	6.81%
L	4	S	8x10	V	79.37%	9.01%
L	4	S	9x9	H	74.02%	6.61%
L	4	S	9x9	V	75.96%	7.65%
L	4	T	8x10	H	26.14%	13.51%
L	4	T	8x10	V	29.63%	11.66%
L	4	T	9x9	H	23.69%	10.81%
L	4	T	9x9	V	29.93%	13.60%
L	5	R	8x10	H	33.07%	8.68%
L	5	R	8x10	V	30.81%	7.26%
L	5	R	9x9	H	33.41%	9.95%

L	5	R	9x9	V	30.64%	7.09%
L	5	S	8x10	H	35.27%	7.71%
L	5	S	8x10	V	34.55%	7.89%
L	5	S	9x9	H	36.27%	8.22%
L	5	S	9x9	V	35.88%	6.73%
L	5	T	8x10	H	9.68%	4.51%
L	5	T	8x10	V	9.40%	4.88%
L	5	T	9x9	H	9.52%	4.39%
L	5	T	9x9	V	9.61%	4.49%
LN	4	R	8x10	H	77.49%	10.54%
LN	4	R	8x10	V	75.16%	8.40%
LN	4	R	9x9	H	71.89%	11.37%
LN	4	R	9x9	V	74.37%	6.76%
LN	4	S	8x10	H	74.17%	10.40%
LN	4	S	8x10	V	75.12%	6.89%
LN	4	S	9x9	H	68.90%	11.11%
LN	4	S	9x9	V	72.77%	7.72%
LN	4	T	8x10	H	22.85%	11.26%
LN	4	T	8x10	V	24.77%	10.98%
LN	4	T	9x9	H	22.54%	10.55%
LN	4	T	9x9	V	24.81%	11.16%
LN	5	R	8x10	H	64.23%	17.06%
LN	5	R	8x10	V	73.54%	7.49%

LN	5	R	9x9	H	58.87%	15.68%
LN	5	R	9x9	V	68.97%	10.71%
LN	5	S	8x10	H	66.71%	16.41%
LN	5	S	8x10	V	75.79%	7.46%
LN	5	S	9x9	H	62.48%	14.16%
LN	5	S	9x9	V	72.58%	9.91%
LN	5	T	8x10	H	14.46%	6.78%
LN	5	T	8x10	V	19.44%	6.66%
LN	5	T	9x9	H	14.04%	6.90%
LN	5	T	9x9	V	17.55%	6.92%